

**RAC GTPASES IN PROSTATE CANCER EXTRVASATION ACROSS
BONE MARROW ENDOTHELIUM**

by

Surabhi Pathak

A thesis submitted to the Faculty of the University of Delaware in partial fulfillment of
the requirements for the degree of Master of Science in Biological Sciences

Winter 2012

Copyright 2012 Surabhi Pathak
All Rights Reserved

**RAC GTPASES IN PROSTATE CANCER EXTRVASATION ACROSS
BONE MARROW ENDOTHELIUM**

by
Surabhi Pathak

Approved: _____
Dr. Kenneth van Golen, Ph.D.
Professor in charge of thesis on behalf of the Advisory Committee

Approved: _____
Randall L. Duncan, Ph.D.
Chair of the Department of Biological Sciences

Approved: _____
George H. Watson, Ph.D.
Dean of the College of Arts and Sciences

Approved: _____
Charles G. Riordan, Ph.D.
Vice Provost for Graduate and Professional Education

ACKNOWLEDGMENTS

I would like to thank Dr. Kenneth van Golen for being an awesome mentor and giving me the freedom to learn by exploring. I would like to thank Dr. William Cain and Dr. Anja Nohe for their valuable suggestions at all times. My special thanks to Linda Sequeria for the awesome experimental designs. I would also like to thank all the members of van Golen lab for being always so helpful and fun to be with.

I am dedicating this work to my family and my best friend Hasan for their support, encouragement and patience.

TABLE OF CONTENTS

LIST OF TABLES.....	vi
LIST OF FIGURES	vii
LIST OF ABBREVIATIONS.....	ix
ABSTRACT	x
Chapter	
1 INTRODUCTION.....	1
1.1 Prostate cancer extravasation , similarities with leukocyte trans- endothelial migration during inflammation.....	2
1.2 Rho GTPases and Prostate cancer metastases	9
1.3 Hypothesis & Specific Aims	14
2 MATERIALS AND METHODS	15
2.1 Cell Lines and Cell Culture	15
2.2 siRNAs	16
2.3 Reverse Transcriptase and Real-Time Quantitative PCR.....	17
2.4 Tumor Cell Diapedesis Assays.....	18
2.5 Rac GTPase Activation Assay.....	18
2.6 Atomic Force Microscopy (AFM).....	19
2.7 Transendothelial Electrical Resistance (TEER)	20
2.8 Fluorescence-Activated Cell Sorting (FACS) Analysis	21
2.9 Statistical Analysis	21
3 RESULTS.....	23
4 DISCUSSION.....	41

5	CONCLUSION.....	50
	REFERENCES	52

LIST OF TABLES

Table 1.1: (a) Endothelial cell adhesion molecules and leukocyte counter-receptors. (b) Endothelial cell adhesion molecules and cancer cell counter-receptors	4
---	---

LIST OF FIGURES

Figure 1.1	Metastatic Cascade Courtesy : Fidler. Cancer, 5th Ed. New York: Lippincott, 1997	3
Figure 1.2	A comparison between leukocyte and cancer cell extravasation of vascular endothelium.	8
Figure 1.3.	The Rho GTPase activation cycle;	10
Figure 1.4.	The Rho GTPase Subfamily, Homology Tree.	11
Figure 1.5.	Signaling from Rac to the Cytoskeleton.....	13
Figure 3.1	Rac isoform expression and isoform-specific depletion in PC-3 cells.....	23
Figure 3.2	Effect of the RacGEF inhibitor NSC23766 (iRac), siRNA specific for Rac1, Rac3, and RhoG, or scrambled control (siScr) on total Rac activation.	24
Figure 3.3	Depletion of RhoG led to a decrease of total Rac activation in PC-3 cells treated with 100ng/mL CCL2.	25
Figure 3.4	Interaction of prostate cancer cells with bone marrow endothelial cells.....	27
Figure 3.5	Elasticity of the PC-3 cells given as the Young's modulus.	28
Figure 3.6	Elasticity of the BMECs given as the Young's modulus	29
Figure 3.7	Effect of depletion of specific Rac isoforms on diapedesis of PC-3 cells across BMEC monolayer	30
Figure 3.8	Effect of introduction of an RNAi-insensitive Rac3 into siRac3-treated PC-3 cell on PC-3 diapedesis.	31
Figure 3.9	Effect of Rac 1 and RhoG depletion on CCL2 stimulated PC-3 cells diapedesis.	32

Figure 3.10	Measurements of trans-endothelial electrical resistance (TEER) of BMECs after addition of PC-3 cells. BMECs were grown on a monolayer, PC-3 cells were added to the monolayer, and the electrical resistance was measured every 10 min up to 1 h (i) and the final measurement at 24 h (ii).....	33
Figure 3.11	Measurements of trans-endothelial electrical resistance (TEER) of BMECs after addition of PC-3 cells. BMECs were grown on a monolayer, PC-3 cells were added to the monolayer, and the electrical resistance was measured at different time points till 30 min.....	34
Figure 3.12	Effect of Rac-1 depletion from BMEC on TEER changes following addition of PC-3 cells.	35
Figure 3.13	Effect of Rac 1 depletion from PC-3 cells on transendothelial electrical resistance (TEER) of BMEC following addition of PC-3 cells.....	36
Figure 3.14	Effect of Rac-3 depletion from BMEC on transendothelial electrical resistance (TEER) changes following addition of PC-3 cells.....	37
Figure 3.15	Effect of addition of Rac-3 depleted PC-3 cells on transendothelial electrical resistance (TEER) changes of BMEC monolayer.....	37
Figure 3.16	Effect of RhoG depletion from BMEC on trans endothelial electric resistance (TEER) changes following addition of PC-3 cells.....	38
Figure 3.17	Effect of addition of RhoG depleted PC-3 cells on trans endothelial electric resistance (TEER) changes of BMEC monolayer.....	39
Figure 3.18	Effect of addition of PC-3 cells on trans endothelial electric resistance of MDCK monolayer.....	40

LIST OF ABBREVIATIONS

BMEC	Bone Marrow Endothelial Cells
PC-3	Prostate Cancer cell line
Rho GTPase	Ras Homology GTPase
Rac-1	Ras-related C3 botulinum toxin substrate 1
Rac-2	Ras-related C3 botulinum toxin substrate 2
Rac-3	Ras-related C3 botulinum toxin substrate 3
RhoG	Ras-Homology Growth-related
ICAM	Inter-Cellular Adhesion Molecule
VCAM	Vascular Cell Adhesion Molecule
DOCK	Dedicator of CytoKinesis
CCL-2	Chemokine Ligand -2
PCNT-1	Pericentrin-1
TEM	Transendothelial Migration

ABSTRACT

Prostate cancer metastasis to bone is the leading cause of morbidity and mortality in men with this disease. One of the crucial steps in the metastatic cascade is the extravasation of the cancer cell across bone marrow endothelium into the bone stroma which can be compared to leukocyte diapedesis across vasculature during inflammation. Rho GTPases are monomeric small GTPases that regulate cytoskeleton and have been shown to play a vital role in prostate cancer metastases by regulating cell morphology and motility. Over expression of RhoC has been reported in prostate cancer cell line PC-3 where it was shown to be important for invasion. Our lab has previously shown that down regulation of RhoC in PC-3 cells results in the morphological changes reminiscent of epithelial to mesenchymal transition with changes in lamellopodia formation attributed to increased activation of Rac GTPases. At the same time, down regulation of Rac GTPase using siRNA resulted in decreased ability of PC-3 to undergo diapedesis across bone marrow endothelium suggesting its role during this process. Rac GTPase branch of Rho subfamily of monomeric GTPases is comprised of four members i.e. Rac1, Rac2, Rac3 and RhoG. The specific roles played by these individual Rac isoforms in prostate cancer skeletal metastases has not been studied forming the basis of the current study and the aim was to identify specific

roles played by these isoforms in PC-3 diapedesis across bone marrow endothelium . Rac1 GTPase was found to be the predominant Rac-isoform in PC-3 cells and is important in mediating binding interactions with BMECs. It was found that Rac 1 can be activated through direct activation of Rac GEFs or indirectly through hierarchical activation of RhoG. Chemokine CCL2 secreted by BMEC can also cause activation of Rac 1 through activation of PCNT1, a novel actin regulating protein, which sequentially interacts with Rho GEFs and DOCK-180 ELMO. Rac1 in BMECs presumably facilitates expression of ICAM-1 levels and interactions with β 1 integrin on PC-3. Reciprocal relationship between Rac 1 and Rac3 was noted in that down regulation of Rac3 increased Rac1 activation levels in PC-3 . Rac 1 was found to promote PC-3 diapedesis and its down regulation led to decrease in diapedesis while down regulation of Rac 3 resulted in an increase in diapedesis presumably through increase in Rac1 levels. Rac-1 maintains BMEC monolayer integrity and it's down regulation results in increase in permeability while down regulation of Rac3 or RhoG does not affect permeability of BMEC. PC-3/endothelial interactions appear to be endothelium specific with decreased permeability observed on interactions with BMEC while no affect on permeability was noted on interaction with MDCK cells.

Chapter 1

INTRODUCTION

Prostate cancer is the most common cancer and second leading cause of death in men in United States accounting for 28% of newly diagnosed cancers in 2010. Only a small proportion of the newly diagnosed prostate cancer causes death with majority of the patients dying of other co-morbid conditions.(1,2) However 90% of patients who die of prostate carcinoma have advanced metastases, to bone in particular, which is the most common cause of morbidity in these patients as well. Metastases to bone results in complications such as compression fracture, bone pain, spinal cord compression, bladder incontinence and symptomatic hypercalcemia. In spite of these debilitating complications experienced by these patients there has not been many therapeutic advances targeted to prevent these lesions from occurring. The current treatment protocols for complications arising from skeletal metastases are mostly palliative in nature and include pharmacological management of bone pain, hormonal therapy, radiotherapy for spinal cord compression, biphosphonates to inhibit osteoclastic activity. It is necessary that the intricacies of the skeletal metastases be understood to identify molecular targets for development of new treatment protocols.

(3-7)

1.1 Prostate cancer extravasation , similarities with leukocyte trans-endothelial migration during inflammation

In order for a tumor cell to undergo metastases it needs to successfully undergo a series of steps which include local tumor invasion by detachment from primary tumor and degradation of the host stroma , entry into the vasculature , survival in the vasculature followed by successful extravasation into the secondary site and colonization at the secondary site by undergoing various adaptive changes (Figure 1). In the context of prostate carcinoma skeletal metastases , the tumor from the prostate invades locally and enters Batson's venous plexus and reaches bone marrow where it extravasates across bone marrow endothelium into the bone stroma interacting with the microenvironment and forming a secondary tumor. Prostate cancer's preferential metastases to bone has been variously attributed to the presence of Batson venous plexus carrying the cancer cells to the axial skeleton where red marrow is abundant and to the preferential interaction of cancer cells with the human bone marrow endothelium and the micro-environment in the bone that favors its further growth (Paget's seed and soil theory) (8-11). Many of the steps in the process of Prostate cancer metastasis are well studied, however, not much is known about the factors mediating the step wherein the tumor cell extravasates across the bone marrow endothelium.

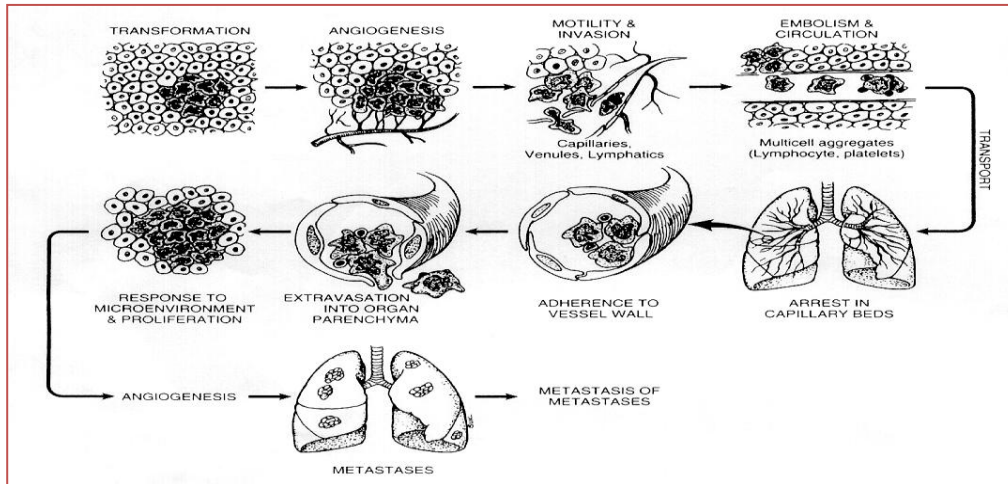


Figure 1.1 Metastatic Cascade Courtesy : Fidler. Cancer, 5th Ed. New York: Lippincott, 1997

The specific step where a prostate cancer cell extravasates across the bone marrow endothelium involves multiple sub-steps that include tumor cell arrest, binding and adhesion to the bone marrow endothelial cell, spreading on the bone marrow endothelial cells, and migration through the endothelial layer followed by invasion into bone stroma. This mimics leucocytes extravasation through vasculature during inflammatory immune response (12). Both leucocyte extravasation and tumor diapedesis involve interactions with endothelium, also, leucocytes and cancer cells express similar surface receptors involved in binding to the endothelial adhesion molecules (Table 1.1) (12).

**Table 1.1(a) Endothelial cell adhesion molecules and leukocyte counter-receptors.
(b) Endothelial cell adhesion molecules and cancer cell counter-receptors**

(a) Endothelial cell surface molecule	Leukocyte counter-receptor
Selectins	
E-selectin	PSGL-1; SLeA-, SLeX-glycoproteins
P-selectin	PSGL-1; SLeA-, SLeX-glycoproteins
L-selectin	PSGL-1; SLeA-, SLeX-glycoproteins
Immunoglobulins	
ICAM	α L β 2 (LFA-1); α M β 2 (Mac-1)
VCAM	α 4 β 1 (VLA-4)
JAM	α L β 2
MadCAM	α 4 β 7
PECAM	α v β 3
Integrins	
α v β 3	L1
α 5 β 1 (VLA-5)	L1
(b) Endothelial cell surface molecule	Cancer cell counter-receptor
Selectins/lectins	
E-selectin	SLeA-, SLeX-glycoproteins
P-selectin	SLeA-, SLeX-glycoproteins
Galectin 3	TF-antigen glycoproteins; MUC1
Immunoglobulins	
ICAM	α 4 β 1 (VLA-4); MUC1
VCAM	CD44
L1	α v β 3

Integrins	
$\alpha 4\beta 1$	VCAM; CD44
$\alpha 6\beta 1$	$\alpha 6\beta 1$
	$\beta 4$
Others	
CLCA	$\alpha 6\beta 4$

**Courtesy : Stepping out of the flow: capillary extravasation in cancer metastasis by Fayth*

Miles; Freddie Pruitt; Kenneth Golen; Carlton Cooper published in the journal Clinical and

Experimental Metastasis, 25, no. 4 (2008): 305-324

During inflammation, cytokines released at the site of injury activates endothelium causing expression of selectins which ligates with the different glycoproteins present on leukocyte resulting in formation of loose associations between leukocyte and the endothelium. This further mediates leukocyte tethering and rolling along endothelium. The cytokines released at the site of inflammation and this loose binding of leukocyte with the endothelium causes activation of integrins on the surface of leukocyte which binds with a strong affinity to the endothelium cellular adhesion molecules (CAMs) (12-20).

Following the formation of strong interactions between leukocyte and endothelium , leukocyte can traverse the endothelium by either migrating between endothelial cells (paracellular extravasation) or migration through opening in the endothelial cells (transcellular extravasation) (20-23). Both processes involve cytoskeleton rearrangements in the leukocyte and endothelium. Also involved are disruptions in the cell-cell adherens junctions that create passage for the migration of the leukocyte. Rho GTPases play a critical role in these processes as they regulate

cytoskeleton rearrangements and stability of adherens junctions which are important in maintaining the integrity and regulating the permeability of the vasculature. (24-26)

Rho signaling through Rho effector kinase (ROCK) promotes disruption of adherens junctions while signaling to effector protein Dia, stabilizes the junction. Ligation of integrins $\beta 1$ and $\beta 2$ on leukocyte with endothelial ICAM-1 and VCAM-1 induces RhoA activation via sequestration of Rho-GDP dissociation inhibitor. RhoA activation results in formation of F-actin stress fibers which exert contractile force in the endothelial cells allowing leukocyte to pass through the endothelium (27-34).

Prostate cancer extravasation across bone marrow endothelium is similar to leukocyte extravasation in many aspects. It has been shown that prostate cancer cells bind preferentially to bone marrow endothelial cells compared to other endothelial cell lines such as HUVEC , HAEC , hepatic endothelial cells and bone marrow stroma cells. However the role of tumor cell interactions on tumor extravasation is still not as clear as in leukocytes. Prostate cancer cells are much larger in diameter (around 30 μ) compared to leukocytes (around 8 μ). It is thought that such large tumor cells in narrow diameter capillaries can get mechanically trapped and extravasate while preferential tumor-endothelial interactions further facilitates this process. The large tumor cell size also means that paracellular route of tumor cell migrations is more plausible than transcellular (35-39).

Similar to leukocyte extravasation across vasculature during inflammation, chemokines secreted by endothelium has been shown to be important in tumor extravasation. One such chemokine CCL-2, a member of CC β -2 family , is known to promote leukocyte migration at the site of inflammation . CCL2 has been shown to be

secreted in high levels by HBMEC. It stimulates prostate cancer cell motility and has been proposed to attract the tumor cells to bone marrow endothelium. Like other chemokines, CCL2 promotes tumor cell motility through activation of Rho GTPases and thus actin cytoskeleton rearrangements (40-44). Ligation of CCL2 with its receptor CCR2 on the PCa cell results in clustering of PCNT1, a novel actin regulating protein, and activation of Rac GTPases. Activated Rac GTPases have been shown to promote PCa binding and extravasation through bone marrow endothelium (45).

In summary the similarities between leukocyte extravasation across vasculature during inflammation and PCa cell extravasation across bone – marrow endothelium can be appreciated in Figure 2. As shown in the Figure 2. (A) Leukocyte “docking” or rolling is mediated by binding of mucin-like glycoproteins to selectins on endothelial cells after activation by a local gradient of cytokines. This is followed by “locking” or firm adhesion of the leukocyte to the endothelium through various leukocyte integrins and their respective endothelial counter-CAMs, also mediated by cytokines. The clustering of endothelial CAMs activates RhoA/ROCK signaling and downregulates Rap1 to disrupt adherens junctions and induce reorganization actin filaments, allowing diapedesis of the leukocyte. B) Cancer cells (e.g. breast, colon, prostate, fibrosarcoma) may “dock” to cytokine-activated microvascular endothelium via and corresponding endothelial selectins and Thomsen–Friedenreich (TF)- antigen. “Locking” has been demonstrated in many cancer cell lines and is mediated by binding of various CAMs to their respective endothelial ligands. Cytokines in the microenvironment stimulate adhesion and subsequent transendothelial migration (TEM). Leukocytes present in the

microvasculature can bind cancer cells and facilitate their adhesion to the endothelium. Endothelial retraction is mediated by cytokines that stimulate the production of ROS, which may irreversibly damage the endothelium.

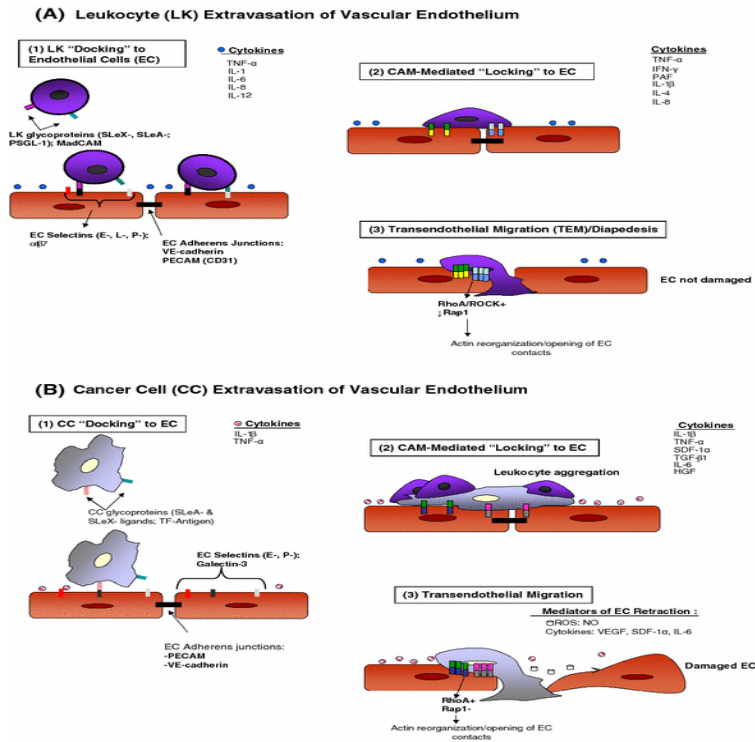


Fig. 1.2 A comparison between leukocyte and cancer cell extravasation of vascular endothelium.

Clustering of CAMs may activate Rho/ ROCK signaling to mediate reorganization of the actin cytoskeleton, and disruption of endothelial junctions facilitating TEM ;

**Courtesy : Stepping out of the flow: capillary extravasation in cancer metastasis by*

Fayth Miles; Freddie Pruitt; Kenneth Golen; Carlton Cooper published in the journal Clinical and Experimental Metastasis, 25, no. 4 (2008): 305-324

1.2 Rho GTPases and Prostate cancer metastases

Rho GTPases are low molecular weight (21-28kDa) members of sub family of super family Ras GTPase of small monomeric GTPases that cycle between active GTP bound state and inactive GDP bound state. Guanine Exchange Factor (GEFs) and GTPase activating proteins (GAPs) regulate the cycle resulting in alternating levels of active form as per cellular needs. These molecular switches convert extracullular signals into multiple cellular activities like cell adhesion, polarity, endocytosis, vesicle trafficking by regulating actin cytoskeleton reorganization (Figure 1.3). As shown in the figure 1.3, Rho GTPase cycle is regulated by molecules such as guanine nucleotide exchange factors (GEFs), GTPase activating proteins (GAPs), and guanosine nucleotide dissociation inhibitors (GDIs). “RXX” is used as a generic representation of any Rho GTPase. They have also been implicated in progression of a cell through cell cycle, differentiation, and oncogenesis and gene transcription (24, 46-48).

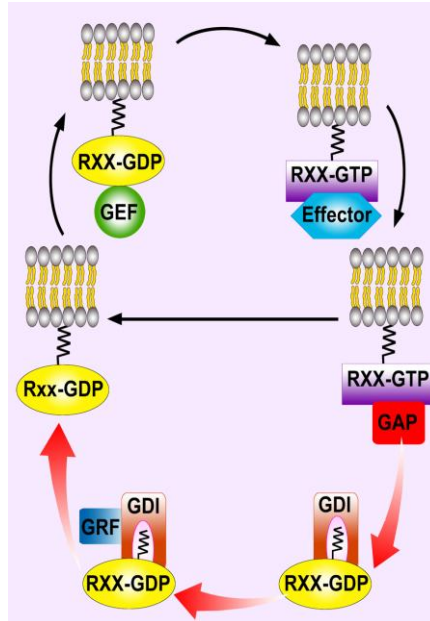


Figure 1.3. The Rho GTPase activation cycle;

* Courtesy : "Rho GTPases in Cancer" Springer Academic Publishers, K.L. van Golen Ed

On the basis of their protein structure the 22 Rho family members are divided into six branches namely the RhoA related, the Rac -1 related, the Cdc42 related, the Rnd –related, the RhoBTB and the Miro sub-family (Figure 1.4). In addition RhoD, Rif and TTF/RhoH do not fall into any of the sub-families. This study focuses exclusively on the members of Rac branch of the family (49).

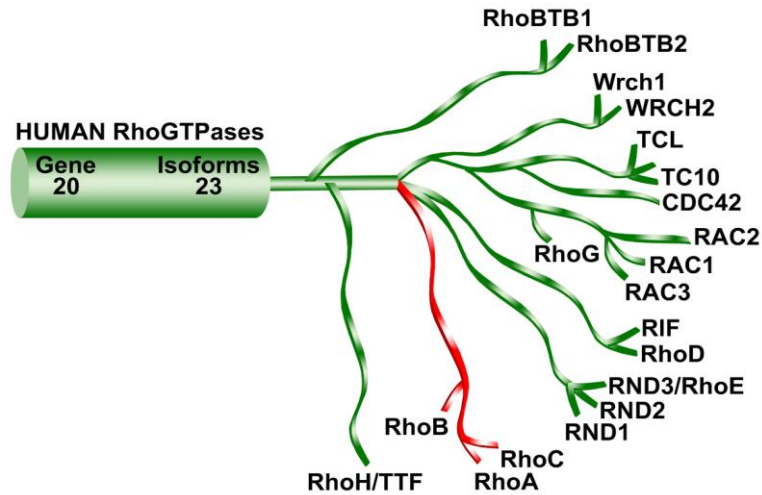


Figure 1.4. The Rho GTPase Subfamily, Homology Tree.

* *Courtesy: "Rho GTPases in Cancer" Springer Academic Publishers, K.L. van Golen Ed*

Rho GTPases have been implicated in cancer progression by facilitating invasion and metastases through regulation of actin cytoskeleton and thus cell motility (50). In the context of prostate cancer, over-expression and activation of RhoC is reported in prostate cancer cell line PC-3 where it plays an important role in invasion but not motility (51, 52). It has been shown that activation of RhoC is through integrin ($\alpha2\beta1$) mediated pathways stimulated upon binding of cancer cell to collagen-1 present in the bone. When RhoC was down regulated in prostate cancer cell line there was a decrease in invasion and experimental metastases. Inhibition of RhoC also caused an increase in random motility in response to IGF-1 stimulation along with morphological changes and alterations in expression of focal adhesion-related proteins (55, 56). Concurrently there was increase in active levels of Rac GTPase promoting linear motility. Further it was shown that down regulation of Rac GTPase caused

decrease in tumor diapedesis (53, 54) which is similar to the role played by Rac GTPases during leukocyte extravasation during inflammation. Thus while RhoC was shown to confer prostate cancer invasive properties it became apparent that Rac GTPases play an important role in facilitating cancer extravasation across bone marrow endothelium. However, Rac GTPase branch of the family is comprised of four isoforms and the specific role played by the individual Rac isoforms in prostate cancer extravasation across bone marrow endothelium is not known. This forms the backdrop of the current study where we attempt to understand the importance of each of the Rac-GTPase isoform in the process of prostate cancer diapedesis.

As mentioned above, Rac GTPase branch of the family is comprised of four isoforms namely Rac-1, Rac-2, Rac-3 and RhoG GTPase (49, 51, and 57). Rac-2 and Rac-3 share a sequence identity of 88 % with Rac-1 while RhoG is 72 % similar. (52,58). Rac-1 is ubiquitous and its deficiency is lethal during embryonic development. Rac-2 is found in hematopoietic cells and its deficiency results in lymphocytic and phagocytic defects. RhoG is found in most of the tissues while Rac-3 is highly expressed in neural tissue (53). RhoG has been shown to be expressed during cell division (58-60). All the Rac-GTPases are involved in lamellopodia formation, membrane ruffling and regulation of cadherin mediated cell-cell adhesion. These actions are mediated through activation of PI-5 kinase and generation of PIP2 causing exposure of barbed or presumably through interaction with the PIR121-Nap125-HSPC300-WAVE complex (61- 65) (Figure 1.5). Additionally, RhoG GTPase has been shown to share some common upstream and downstream regulatory proteins with Rac-1 GTPase such as Vav2 (67). Activation of RhoG can lead to activation of Rac-1

through interaction with Dock180- ELMO providing alternate way of activation of Rac-1 other than through direct activation of Rac GEFs (68, 69).

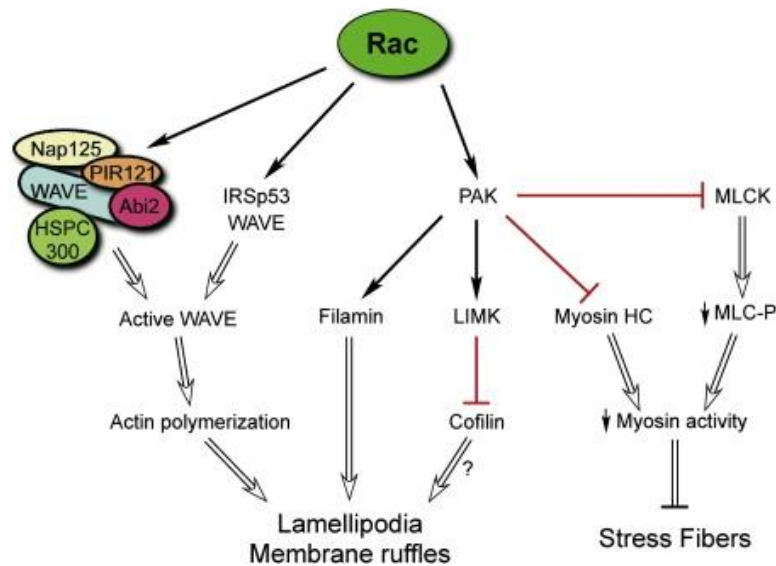


Figure 1.5. Signaling from Rac to the Cytoskeleton.

The pathways leading from Rac activation to the formation of lamellipodia and membrane ruffles, and the loss of stress fibers, are described in the text. Direct activating signals are presented by solid arrows. Inhibitory signals are depicted as red bars. Double-lined arrows and bars represent the net result of a signaling pathway. Abbreviations used: PAK, p21-activated kinase; LIMK, LIM kinase; MLCK, myosin light chain kinase.

* Courtesy : "Rho and Rac Take Center Stage," by Keith Burridge, Krister Wennerberg , which appeared in the journal Cell, Volume 116, Issue 2, 23 January 2004, Pages 167-179)

Rac GTPase have been implicated in tumor invasion and metastases through their regulation of cytoskeleton. Deregulated expression, but not mutations, of

Rac GTPase has been observed in many cancers. Rac-1 , Rac -2 and RhoG are overexpressed in breast cancer while colon cancer is associated with increased expression of Rac-1 and brain tumors with increased expression of Rac-3 GTPase(64,65). Rac-1 and Rac-3 GTPase have been found to be overexpressed in prostate cancer and high-grade prostatic intraepithelium neoplasia suggesting its role in the cancer development and progression (66). Thus it appears that Rac GTPase plays a role in tumorigenesis and metastases of a variety of cancers but the extent of their significance is not fully known. This study was carried out to investigate further the role of specific Rac isoforms in prostate cancer metastases specifically diapedesis across bone marrow endothelium, using PC-3 cell line. Following are the hypothesis and the specific aims that the study aimed to address.

1.3 Hypothesis & Specific Aims

Hypothesis: Individual Rac isoforms have specific role during PC-3 diapedesis across bone marrow endothelium

Aim 1: To understand the interplay, if any, between the Rac isoforms and the effect of chemokine CCL2 secreted by BMEC in modulating the activation levels of Rac1 GTPase in PC-3 cells.

Aim 2: To understand the role of Rac isoforms in mediating interactions between PC-3 cells and BMECs.

Chapter 2

MATERIALS AND METHODS

2.1 Cell Lines and Cell Culture

PC-3 PCa cell lines were obtained from American Type Culture Collection (Manassas, Va) and maintained in Ham's F-12 medium with 1.5 g/L sodium pyruvate, 2 mM L-glutamine, and 10% FBS (Invitrogen/Gibco, Carlsbad, Calif). C4-2 cells were a gift from Dr. Robert Sikes (University of Delaware) and maintained in T-medium containing 10% FBS (Invitrogen/Gibco). Human bone marrow endothelial cells (BMECs) were a gift from Dr. Graca Almeida-Porada (University of Nevada School of Medicine, Reno, Nevada). Madin Darby canine kidney (MDCK) cells were maintained in DMEM supplemented with 10% fetal bovine serum, penicillin, and streptomycin. PC-3 and BMECs were maintained in Medium 199 with Earle's salts, L-glutamine, 2,200 mg/L sodium bicarbonate, 25 mM HEPES (Invitrogen/Gibco) buffer, 10% FBS, 1% pen/strep, endothelial cell growth supplement (BD Biosciences, Bedford, Mass), and 7500 u/500 mL media of heparin (Sigma-Aldrich, St. Louis, Mo). All cell lines were maintained at 37°C in a 90% : 10% air : CO₂ incubator. C3 exotransferase was introduced into cells as previously described using a lipid transfer-mediated method (70) and treated for 2 h before analysis. Rac1 inhibitor NSC23766 (Calbiochem, San Diego, Calif) treatment was performed by adding directly to tissue culture medium to a final concentration of 100 μM 1 h prior to analysis. Prostate cancer cells were

stimulated with 100 ng/mL recombinant human (rh)CCL2 (MCP-1) in tissue culture medium (Millipore-Chemicon Inc., Billeceria, Mass) for 30 min during the Rac activation assays and kept in the presence of the chemokines during the diapedesis assays.

2.2 siRNAs

Specific siRNAs for human Rac1 and Rac3 GTPases were a gift from Dr. Marc Symons and described previously (71). RhoG siRNA and scrambled control siRNAs were synthesized by integrated DNA technologies. RhoG siRNA target sequences were (1) 5'-TGCCCTGATGTGCCCATCCTGCTGGTGGG-3' and (2) 5'-ACGTGCCTGCTCATCTGCTACACA ACTAA-3'. The Rac1, Rac3, and RhoG siRNA duplexes were formed by adding 30 μ L of each RNA oligo solution together with 15 μ L of 5x annealing buffer (100 mM NaCl and 50 mM Tris-HCl pH 7.5) to give a final volume of 75 μ L and a final concentration of 20 μ M; incubated for 2 min in water bath at 95°C; allowed to cool to room temperature. Additional experiments were performed using ON-TARGET plus SMARTpool siRNAs Rac1, Rac3, and RhoG siRNAs that were obtained from Dharmacon (Dharmacon/Thermo Scientific, Lafayette, Colo). siRNAs were transfected into prostate cancer cells using FuGene6 (Roche, Indianapolis, Ind) or GeneSilencer Reagent (Genlantis, San Diego, Calif) per the manufacturers instructions and cells used 72 h after transfection. For rescue experiments, mutations were generated using the QuickChange II Site-Directed Mutagenesis kit (Stratagene) according to the manufactures recommendations. To fully abolish the effect of siRNAs, two nucleotides in the siRNA-targeted area were

changed in both Rac3 and RhoG GTPases. To create a RhoG fast cycling mutant, glutamine 63 was converted to lysine.

2.3 Reverse Transcriptase and Real-Time Quantitative PCR

Total RNA was harvested from cells and converted to cDNA as previously described (52). PCR primers were designed using the primer design feature on the Evocycler PCR program (Evogen Ltd., UK). Primer design parameters were set to optimally produce PCR products between 100 and 150 bp in size. Primer sequences are found in Supplemental Table 1 (see Table 1 in Supplementary Material available online at doi:10.1155/2011/541851). RT-PCR was performed on an Evocycler EPx (Evogen Ltd.) using Fast SYBR Green chemistry (Applied Biosystems Inc., Foster City, Calif) per the manufacturers recommendations for 30 cycles (98°C for 15 s, 67°C for 15 s, and 72°C for 30 s), and PCR products visualized on a virtual gel and band intensities were normalized to GAPDH using the Evocycler PCR program.

For quantitative (q)PCR, RNA was isolated from the cell lines using TRIzol Reagent (Invitrogen, Carlsbad, Calif). cDNA was synthesized from this RNA using the Promega Reverse Transcription kit (Promega Corp., Madison, Wis). Appropriate primers (Integrated DNA Technologies, Inc., Coralville, Iowa) were diluted to a final concentration of 10 μ M. The cDNA synthesized from the isolated RNA was diluted to a final concentration of 4 ng/ μ L. Reactions were prepared as a bulk “master mix” using the ABI SYBR Green PCR Master Mix (Applied Biosystems Inc., Foster City, Calif) for each target gene/primer pair used. Three no-template controls were included for each primer pair being used. A 5 μ L aliquot of cDNA was

pipetted into each well of the ABI 96-well plate, and 20 μ L of the reaction master mix was added to it. Plates were covered with ABI adhesive cover, centrifuged at 1000 rpm to mix the contents, and run on an ABI 7000 real-time qPCR machine housed in the Center for Translational Cancer Research (University of Delaware).

2.4 Tumor Cell Diapedesis Assays

Tumor cell diapedesis assays were performed as previously described (54). Briefly, 100,000 HBME cells were added to the top chamber of either uncoated or Matrigel-coated Transwells 24 h prior to the assay and allowed to form a confluent monolayer. PC-3 and C4-2 cells were harvested, labeled with Calcein AM (Invitrogen/Molecular Probes) per manufacturers recommendations, and resuspended in serum-free medium containing 0.1% BSA at a concentration of 3.75×10^5 cells/mL, and 0.5 mL was added to the top chambers. The chambers were incubated for 24 h at 37°C in a 10% CO₂ incubator. Medium was aspirated from the top chamber, and excess Matrigel and cells were removed from the filter using a cotton swab. Filters were cut away from the inserts, mounted on microscope slides, and visualized on a fluorescent microscope and number of invaded cells counted.

2.5 Rac GTPase Activation Assay

Activation of total Rac GTPase proteins was performed using a GLISA pan-Rac activation assay kit (Cytoskeleton Inc., Denver, Colo) as previously described (54). Briefly, prostate cancer cells were grown to 75% confluence in a 100 mm dishes and serum starved for 24 h. On the day of the assay, cells were harvested using nonenzymatic cell dissociation buffer (Sigma-Aldrich), washed twice with ice-cold

PBS, and resuspended in 65 μ L GLISA lysis buffer. Protein lysates were transferred to ice-cold 1.5 mL centrifuge tubes and clarified by centrifugation at 10,000 rpm for 2 min. Protein concentrations were determined using the supplied Precision Red advance protein assay and 1.0 mg/mL protein used for the GTPase activation assay per manufacturers recommendations. After antibody and horseradish peroxidase detection reagent incubation, signals were detected on a Benchmark Plus microplate spectrophotometer at 490 nm (Bio-Rad Laboratories, Hercules, Calif).

2.6 Atomic Force Microscopy (AFM)

All AFM experiments were conducted with a Bioscope II (Veeco, Santa Barbara, Calif) using silicon-nitride tips (Veeco; spring constant 0.06 N/m). Unbinding force measurements were conducted with tips functionalized with collagen or fibronectin (Becton-Dickinson, Franklin Lakes, NJ) at concentrations of 50 μ g/mL and 15 μ g/mL, respectively. Likewise, 35 mm tissue culture dishes (Corning Inc., Corning, NY) were coated with collagen or fibronectin and sterilized under ultraviolet light overnight. PC-3 cells were transfected with siRNA specific for Rac1, Rac3, or RhoG using FuGene6 (Roche) or GeneSilencer Reagent (Genlantis) and plated on the prepared dishes 8 h prior to experimentation. BMECs were cultured in RPMI 1640 media (Hyclone/Thermo Scientific) supplemented with 10% FBS. The functionalized AFM tip was dropped onto a single live BMEC cell and after attachment was verified, the loaded tip was gently lowered onto the center of a PC-3 cell. The unbinding force interaction between the two live cells was measured. The unbinding force is the force required to separate two adhesion molecules and is measured in piconewtons (pN).

The number of events for a particular unbinding force is the number of molecules separated at each force. Specifically, 250 unbinding events were captured per cell site with 4 areas probed per cell, and 3 separate cells were probed per treatment. Force curves were generated at a frequency of 1 Hz in a relative trigger mode.

AFM stiffness measurements were based on recording the elastic response of cells, BMECs and PC-3s using an AFM tip. The AFM was operated in the force-volume mode for recording a set of loading/unloading load displacement curves at a frequency of 1.03 Hz and a forward/reverse velocity of 4.11 $\mu\text{m}/\text{sec}$. The resultant measurement is the dynamic elastic modulus (a.k.a. the Young's modulus), which measures the stiffness of the cell. The Young's modulus is the ratio of stress to strain and is thus represented by units of pressure, Pascals (Pa). Cell stiffness changes are due to morphologic changes resulting from alterations in cytoskeletal structure [reviewed in (78)]. The elastic modulus was measured with individual BMECs, individual PC-3 cells, and the duo: PC-3 cells attached to plated BMECs and BMECs attached to plated PC-3 cells. The elastic modulus for the BMEC/PC-3 combinations was generated for the plated cell, and the attached cells separately. Each force-volume map consists of 256 data points per sample site with 3 separate sites measured per experimental condition, 3 separate times.

2.7 Transendothelial Electrical Resistance (TEER)

Transendothelial electrical resistance (TEER) measurements were done using Epithelial Voltohmmeter (EVOM; World Precision Instruments Inc., Sarasota, Fla) following manufacturers directions. Briefly, BMECs were plated at a concentration of 1.3×10^6 cells/mL on 12-well 0.4 μ polycarbonate membrane inserts (CLS3401; Corning Transwell) and were maintained until day 4 (we determined empirically that

the TEER for the BMEC monolayer was optimum on day 4 after plating due to maturation of cell junctions). On day 4, tissue culture medium was removed from the top chamber, an equal concentration of PC-3 cells was added to the BMEC monolayer and TEER measured at specified intervals.

2.8 Fluorescence-Activated Cell Sorting (FACS) Analysis

Prostate cancer cells were cultured in T25 flasks (Corning Inc., Edison, NJ), detached, washed, and resuspended in 5% bovine serum albumin (BSA; Sigma-Aldrich) in phosphate buffered saline (PBS; Sigma-Aldrich). All washes and resuspensions were also performed in 5% BSA containing PBS. One set of control and siRac1-transfected prostate cancer cells were each further treated with CCL2 (100 ng/mL) for 30 min, washed, and resuspended. The several states of β 1 activation were queried with two conformation-sensitive antibodies N29 (BD Biosciences, Franklin Lakes, NJ) and HUTS-21 (BD Biosciences) in addition to a total β 1 conformation-insensitive antibody, MAR4 (Chemicon, Billerica, Mass). All antibodies were used at a final concentration of 10 μ g/mL, and all incubations were conducted in the dark and at 37°C. Cells were analyzed using an FACS Calibur cytometer (BD Biosciences), equipped with 488 nm and 633 nm lasers. Analyses were performed on 10,000-gated events, and the numeric data were processed with Cellquest software (Becton Dickinson).

2.9 Statistical Analysis

All experiments were performed a minimum of three separate times with individual transfections consisting of no less than three replicates per experiment. Statistical analysis of the combine experiments was performed using GraphPad Prism and by the University of Delaware College of Agriculture and Natural Resources Statistics

Laboratory. A one-way ANOVA analysis was used with Bonferroni's post hoc analysis for comparison between multiple groups. A Students *t*-test was used for comparison between two groups. Significance was defined as a *P* value < .001. Data is represented as mean \pm standard deviation.

Chapter 3

RESULTS

The first step was to understand the relative expression of the Rac isoforms in PC-3 cells at mRNA level. Quantitative PCR was done and the results are shown in the Figure 3.1 below. Rac -1 was found to be the predominant isoform compared to others. Individual siRNAs (1) and (2), specific for Rac1, Rac3, or RhoG, were compared. Messenger RNA was harvested and SYBR green-based qPCR performed using primers specified above. Relative expression levels were normalized to GAPDH expression from the corresponding sample and expressed as arbitrary units (a.u.).

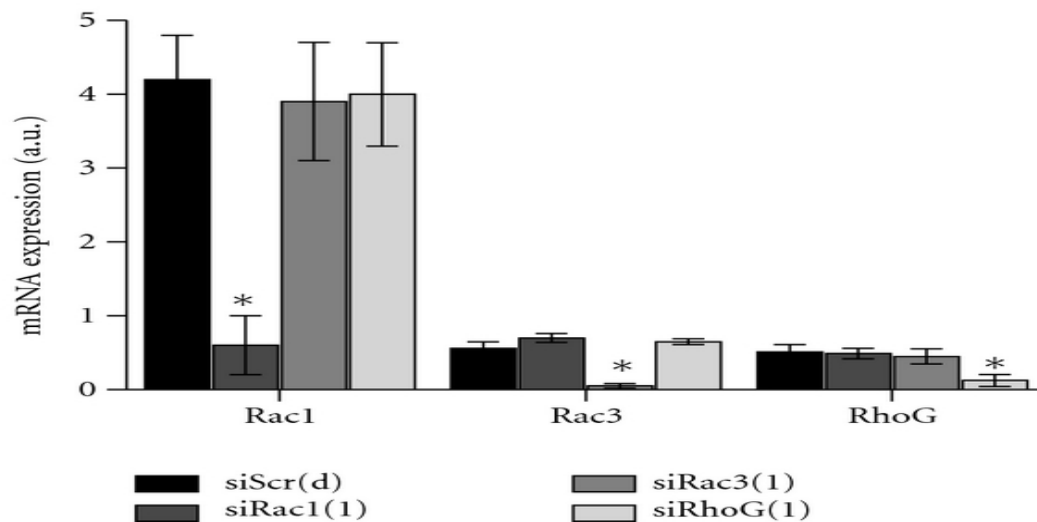


Figure 3.1 Rac isoform expression and isoform-specific depletion in PC-3 cells.

In the next step relative active levels of the Rac isoforms in PC-3 were measured using Rac activation assay. PC-3 cells were depleted of the individual Rac isoform and its effect on total Rac activation level was measured. As can be seen in figure 3.2 depletion of Rac caused the most decrease in total activated Rac levels. Cells were treated with 100 μ M NSC23766 for 1 h or 20 μ M siRac1, siRac3, or siRhoG. Activation of total Rac was performed using GLISA. Cells treated with iRac or transfected with siRNA to Rac isoforms were compared with untransfected (UT) and representative siRNA-scrambled control (siScr). Each analysis was performed in triplicate with individual transfections.

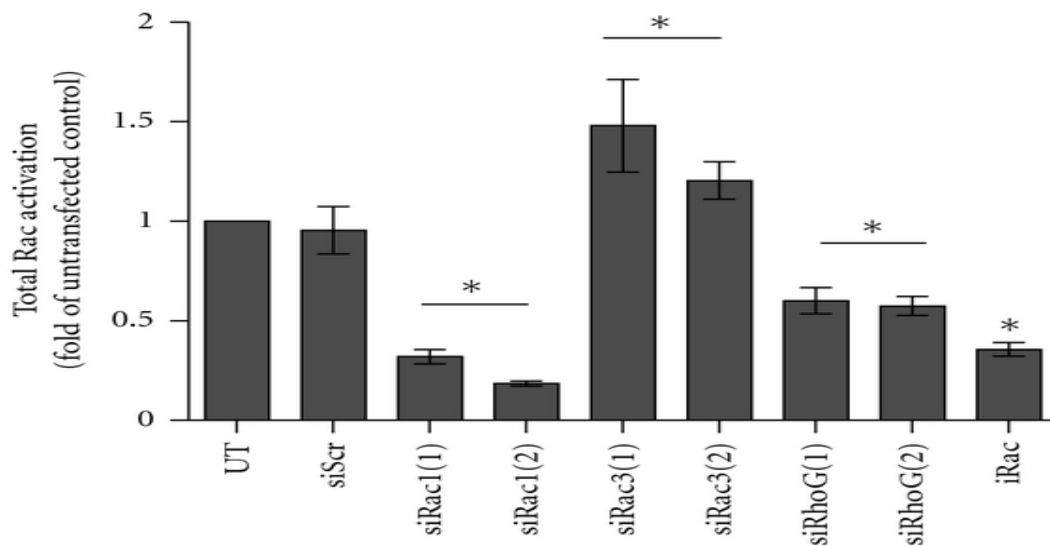


Figure 3.2 Effect of the RacGEF inhibitor NSC23766 (iRac), siRNA specific for Rac1, Rac3, and RhoG, or scrambled control (siScr) on total Rac activation.

To test if RhoG could be acting downstream of CCL-2 in Rac-1 activation, PC-3 cells were depleted of RhoG and Rac activation levels measured on stimulation with CCL2 compared to untreated PC-3 cells. Rescue experiment was performed by introducing siRNA resistant RhoG and Rac activation measured. As can be seen in figure 3.3 depletion of RhoG leads to decreased levels of Rac activation on stimulation with CCL2 compared to untreated. Rescue experiments were performed by introducing a siRNA-insensitive RhoG GTPase. Shown are means \pm S.D. of at least triplicate analysis representing individual transfections, with significance being $P < .001$; (*) signifies a significant difference between siRNA-transfected cells and stimulated controls, while (^) signifies a significant difference between siRNA-transfected and -rescued cells.

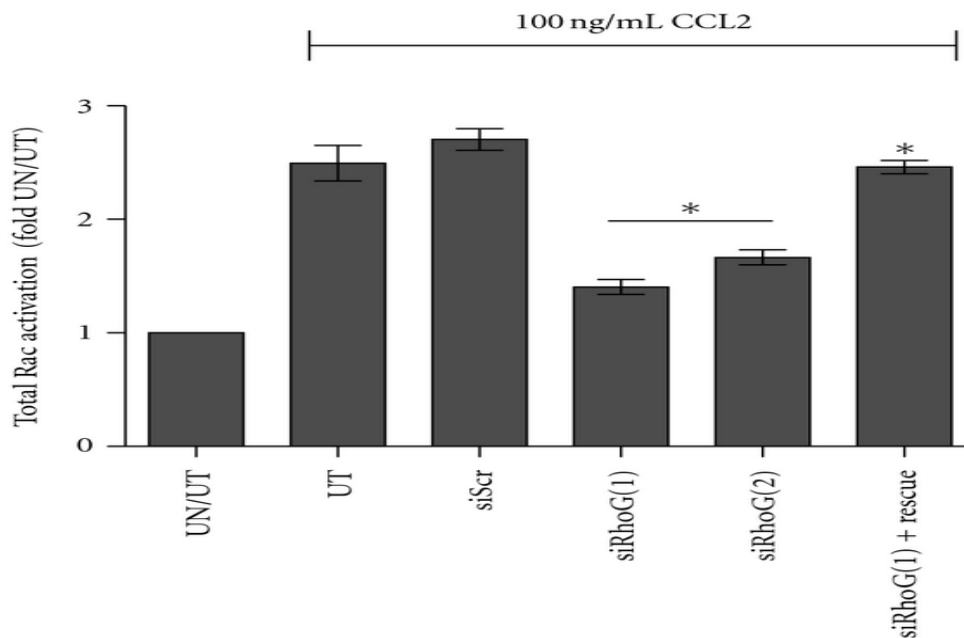
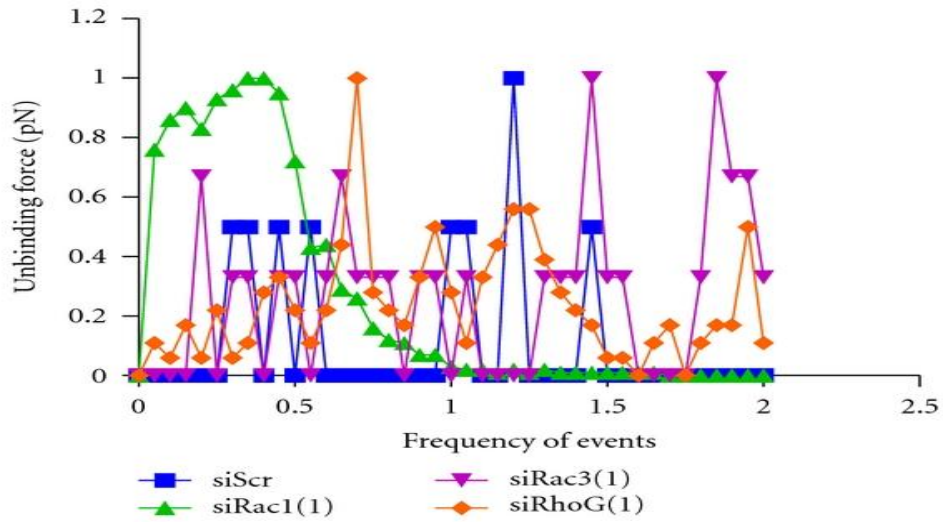
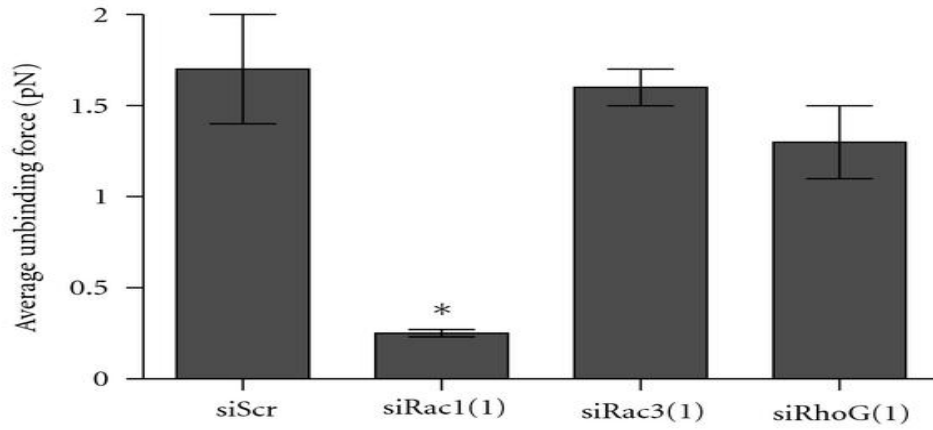


Figure 3.3 Depletion of RhoG led to a decrease of total Rac activation in PC-3 cells treated with 100ng/mL CCL2.

To study the role of Rac isoforms in mediating interaction between PC-3 and BMEC, PC-3 depleted of specific Rac isoforms were plated on top of BMEC and unbinding force measured using atomic force microscopy. As can be seen in figure 3.4 depletion of Rac 1 led to significant decrease in the unbinding force required compared to control while depletion of other isoforms do not seem to cause much change in the unbinding force required. BMECs was attached to the AFM tip and the unbinding forces of PCa cells measured. PC-3 cells were transfected with siRNAs specific for individual Rac isoforms. Shown are the results from one set of siRNAs. Figure 3.4(a) is the effect on the frequency of unbinding events and forces (pN) occurring between BMECs and PC-3 cells after depletion of each Rac isoform. Figure 3.4 (b) is the average unbinding force occurring between BMECs and PC-3 cells. The average unbinding force is the physical force required to pull two adhered cells apart. Data are compiled from 3000 data points and are the mean \pm S.D. with significance being $*P < .001$.



(a)

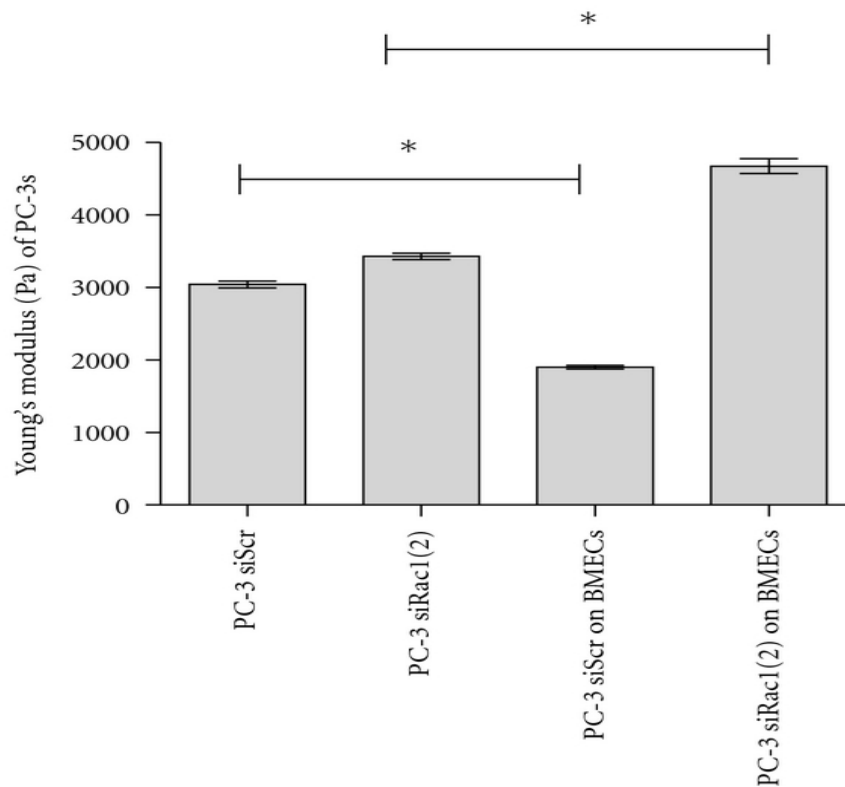


(b)

(Courtesy: Linda Sequeria)

Figure 3.4 Interaction of prostate cancer cells with bone marrow endothelial cells.

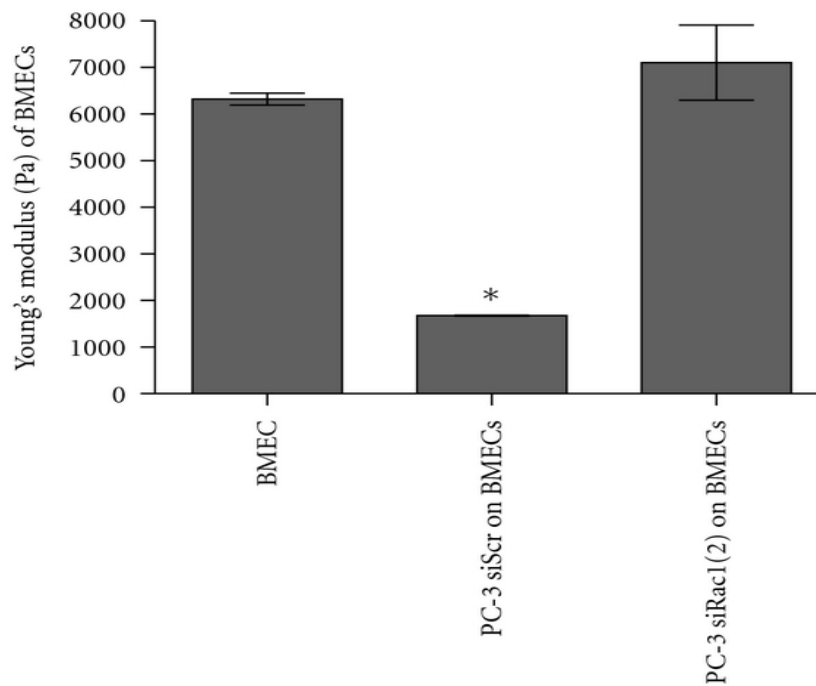
Further, changes in elasticity of BMEC and PC-3 upon their interaction was studied using atomic force microscopy. As can be seen in figure 3.5 interaction of PC-3 with BMEC causes significant increase in elasticity of PC-3 which is inhibited upon depletion of Rac -1 from these cells. Elasticity is a ratio of cell stress and strain and is measured in Pascals. BMECs were grown as a monolayer and control (siScr) or siRac1 expressing PC-3 cells were allowed to bind to the BMEC monolayer.



(Courtesy: Linda Sequeria)

Figure 3.5 Elasticity of the PC-3 cells given as the Young's modulus.

Changes in elasticity of BMEC and PC-3 upon their interaction was studied using atomic force microscopy. As can be seen in figure 3.6 interaction of PC-3 with BMEC causes significant increase in elasticity of BMEC which is inhibited upon depletion of Rac -1 from PC-3 cells. Elasticity is a ratio of cell stress and strain and is measured in Pascals. BMECs were grown as a monolayer and control (siScr) or siRac1 expressing PC-3 cells were allowed to bind to the BMEC monolayer.



(Courtesy: Linda Sequeria)

Figure 3.6 Elasticity of the BMECs given as the Young's modulus .

In the next step, PC-3 cells were depleted of individual Rac isoforms and its effect on diapedesis measured using diapedesis assay. As can be seen in figure 3.7 depletion of Rac -1 led to a significant decrease in PC-3 diapedesis , depletion of Rac-3 resulted in an increased diapedesis. BMECs were layered onto a Matrigel-coated filter and allowed to form a monolayer; 0.5 mL of a suspension of 3.75×10^5 PC-3 cells/mL were added to the BMECs and allowed to undergo diapedesis for 24 h. Treated and transfected cells were compared with untransfected or scrambled controls.

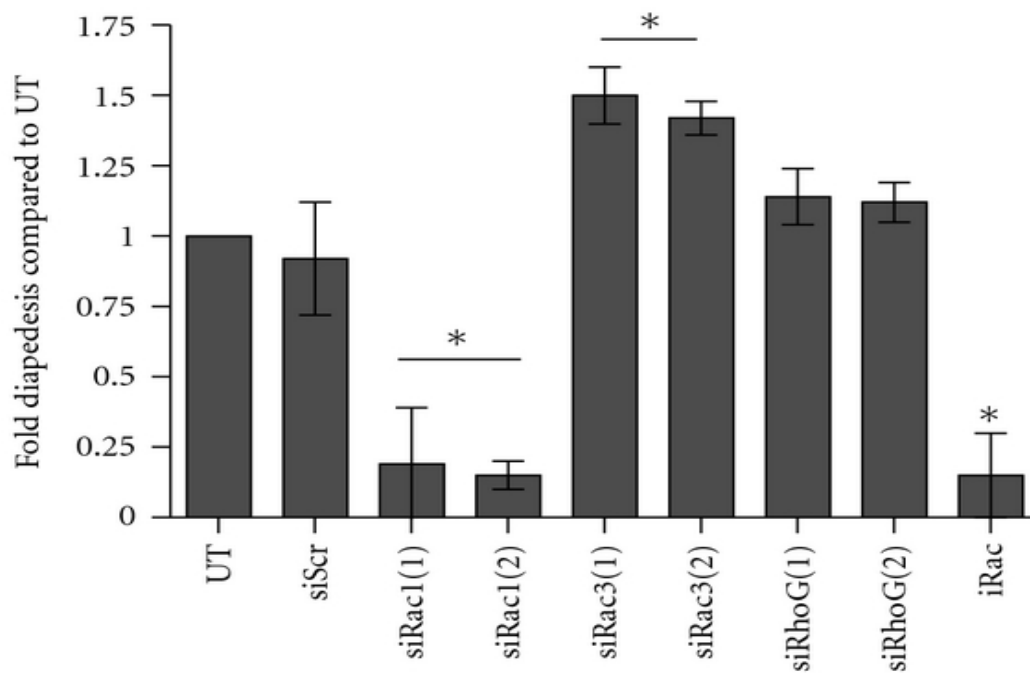


Figure 3.7 Effect of depletion of specific Rac isoforms on diapedesis of PC-3 cells across BMEC monolayer

Shown in figure 3.8 is the effect of rescue of Rac-3 in siRac-3 treated PC-3 on diapedesis across BMEC. Introduction of RNAi-insensitive Rac-3 resulted in the reversal of the increased diapedesis seen upon depletion of Rac-3. RNAi-insensitive Rac3 was introduced into siRac3 transfected PC-3 cells and diapedesis measured. Shown in all four panels is the mean \pm S.D. of at least triplicate analysis with significance being $*P < .001$. Noncapped lines above the bars represent that the siRNA group is significantly different from controls.

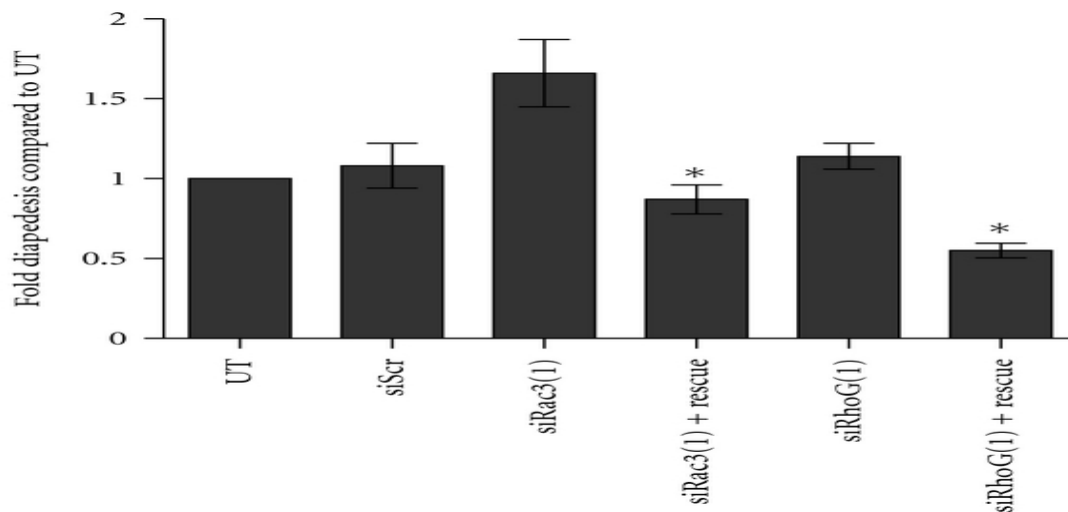


Figure 3.8 Effect of introduction of an RNAi-insensitive Rac3 into siRac3-treated PC-3 cell on PC-3 diapedesis.

Figure 3.9 shows the effect of depletion of Rac isoforms on CCL-2 stimulated diapedesis of PC-3 across BMEC monolayer. As can be seen, depletion of Rac-1 causes significantly lower diapedesis compared to control. Depletion of RhoG also results in a decrease of diapedesis compared to control and the effect is reversed upon introduction of siRNA resistant form of RhoG. PC-3 cells were treated with 100

ng/mL CCL2 in a diapedesis assay. Control untransfected (UT) and siRNA control (siScr) cells demonstrated increased diapedesis compared with untreated/untransfected (UN/UT) PC-3 cells. The ability of cells to undergo CCL2-stimulated diapedesis after depletion of Rac1, RhoG, or treatment with iRac was compared to UT and siScr. Rescue experiments of RhoG-depleted cells were performed by the introduction of a siRNA-insensitive RhoG. Rac1-depleted cells were rescued with the introduction of fast cycling RhoG (RhoGQ63L).

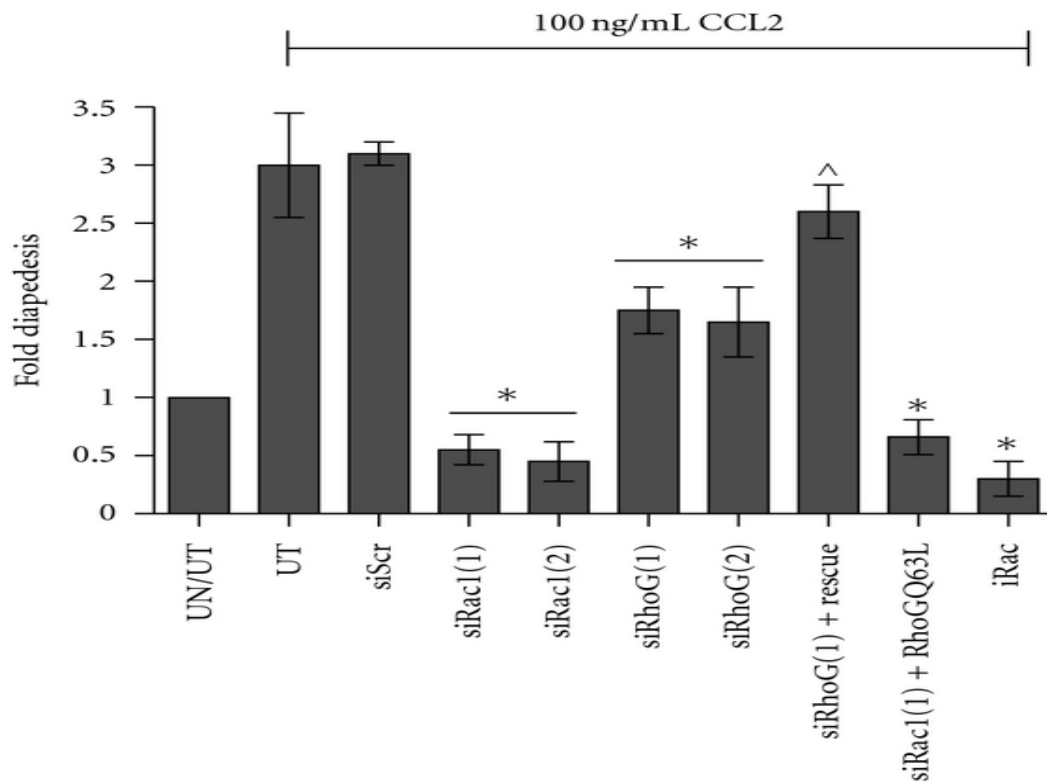


Figure 3.9 Effect of Rac 1 and RhoG depletion on CCL2 stimulated PC-3 cells diapedesis.

Figure 3.10 and 3.11 show changes in transendothelial electric resistance (TEER) measurement across BMEC monolayer on addition of PC-3 cells. TEER is a measurement of permeability of a cell monolayer. As can be seen below addition of PC-3 cells causes a significant decrease in TEER readings compared to control.

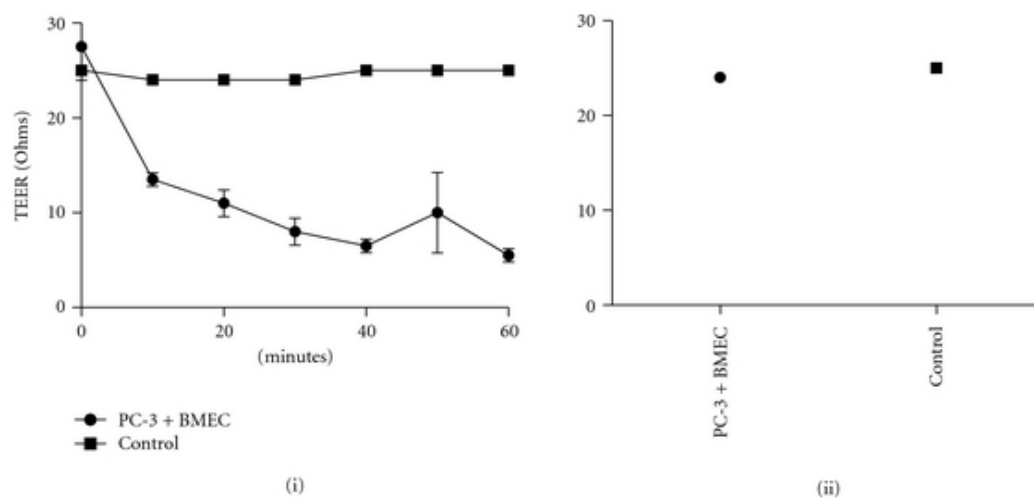


Figure 3.10 Measurements of trans-endothelial electrical resistance (TEER) of BMECs after addition of PC-3 cells. BMECs were grown on a monolayer, PC-3 cells were added to the monolayer, and the electrical resistance was measured every 10 min up to 1 h (i) and the final measurement at 24 h (ii).

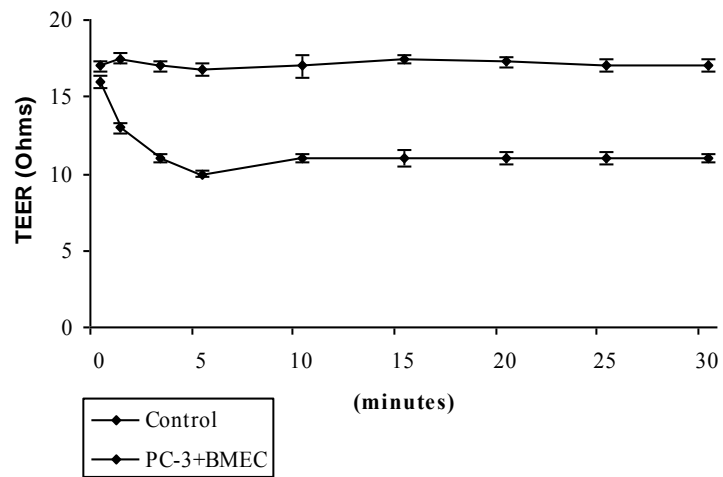


Figure 3.11 Measurements of trans-endothelial electrical resistance (TEER) of BMECs after addition of PC-3 cells. BMECs were grown on a monolayer, PC-3 cells were added to the monolayer, and the electrical resistance was measured at different time points till 30 min.

Figure 3.12 and 3.13 below show the effect of depletion of Rac-1 from PC-3 and BMEC on changes in TEER of BMEC monolayer of addition of PC-3 compared to control. Control and siRac 1 treated BMECs were grown into a monolayer and equal amount of control or siRac-3 treated PC-3 cells were added to the monolayer on day 4 and TEER measured at different time points till 30 min

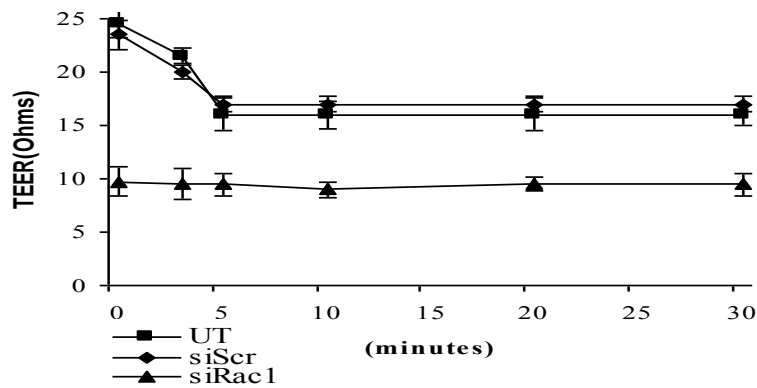


Figure 3.12 Effect of Rac-1 depletion from BMEC on TEER changes following addition of PC-3 cells.

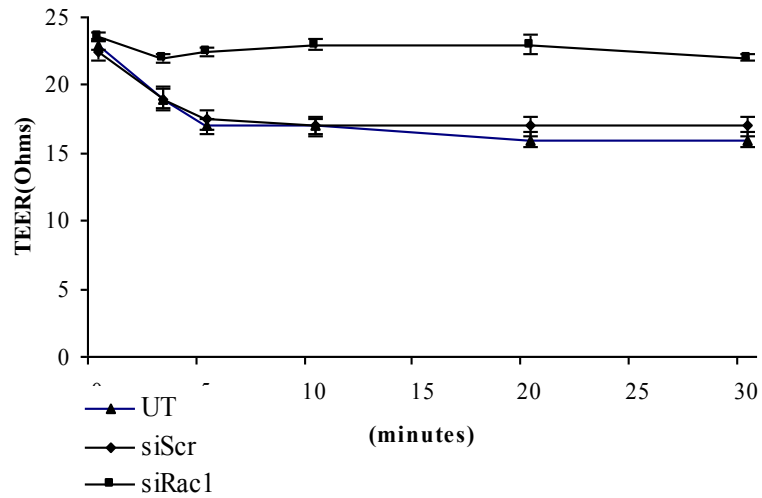


Figure 3.13 Effect of Rac 1 depletion from PC-3 cells on transendothelial electrical resistance (TEER) of BMEC following addition of PC-3 cells.

Figure 3.14 and 3.15 below show the effect of depletion fo Rac-3 from PC-3 and BMEC on changes in TEER of BMEC monolayer of addition of PC-3 compared to control. Control and siRac 3 treated BMECs were grown into a monolayer and equal amount of control or siRac-3 treated PC-3 cells were added to the monolayer on day 4 and TEER measured at different time points till 30 min

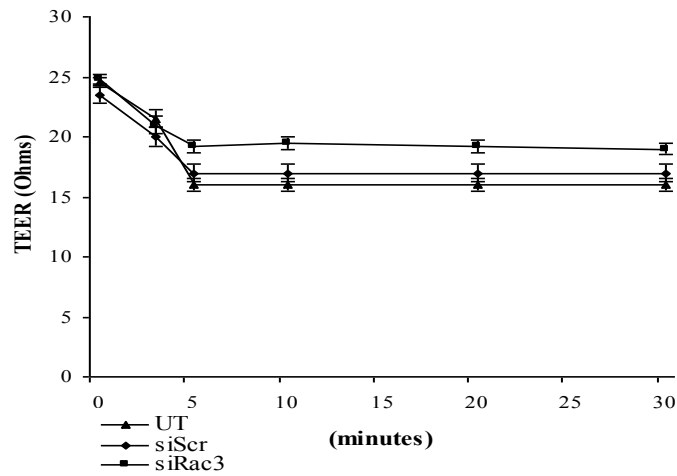


Figure 3.14 Effect of Rac-3 depletion from BMEC on transendothelial electrical resistance (TEER) changes following addition of PC-3 cells

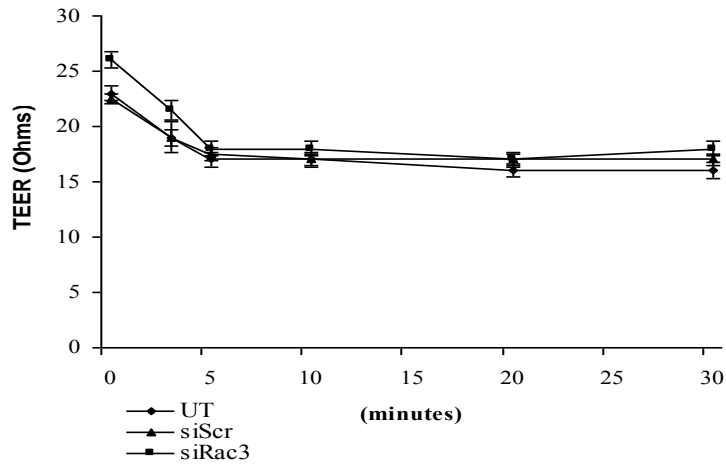


Figure 3.15 Effect of addition of Rac-3 depleted PC-3 cells on transendothelial electrical resistance (TEER) changes of BMEC monolayer

Figure 3.16 and 3.17 below show the effect of depletion fo Rac-3 from PC-3 and BMEC on changes in TEER of BMEC monolayer of addition of PC-3 compared to control. Control and siRhoG treated BMECs were grown into a monolayer and equal amount of control or siRhoG treated PC-3 cells were added to the monolayer on day 4 and TEER measured at different time points till 30 min .

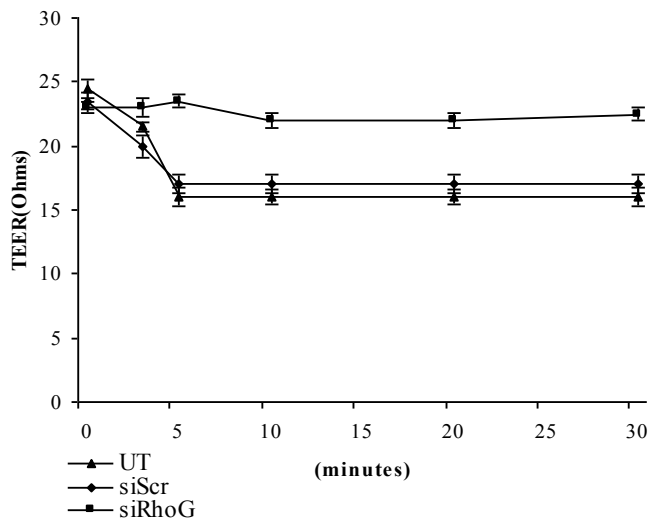


Figure 3.16 Effect of RhoG depletion from BMEC on trans endothelial electric resistance (TEER) changes following addition of PC-3 cells.

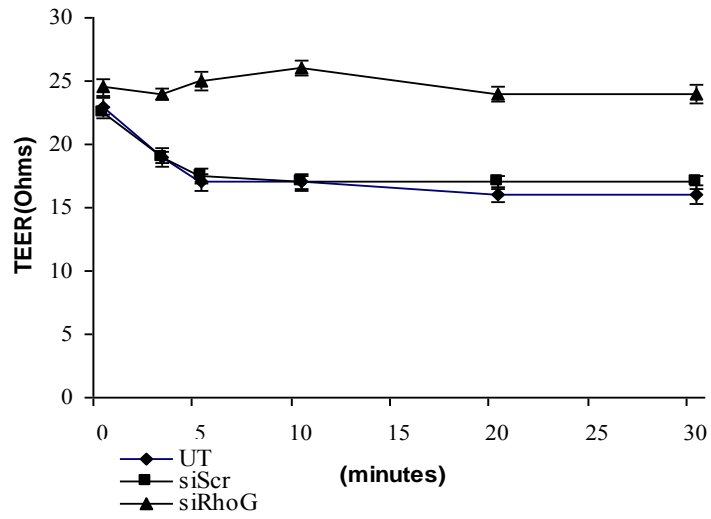
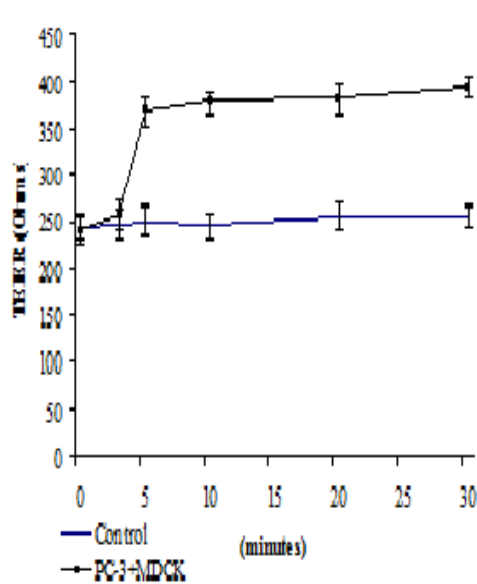
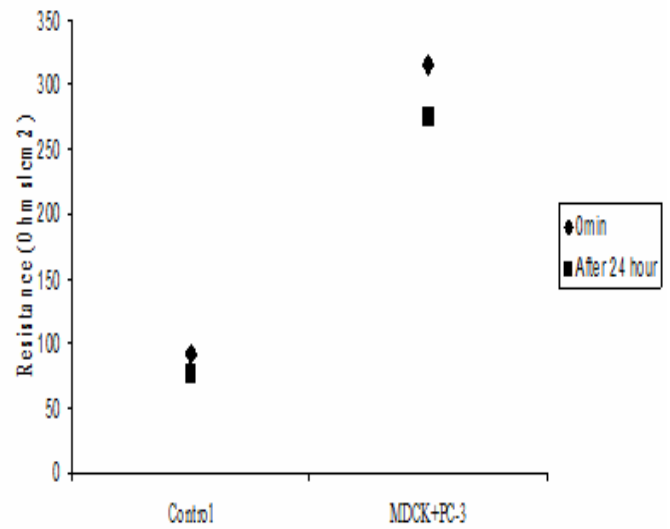


Figure 3.17 Effect of addition of RhoG depleted PC-3 cells on trans endothelial electric resistance (TEER) changes of BMEC monolayer

To study if the effect on transendothelial electrical resistance changes on BMEC monolayer on addition of PC-3 was endothelium specific, PC-3 cells were added on renal epithelial cell monolayer (MDCK) and TEER measured and the results are shown in figure 3.18. MDCK cells were grown on a monolayer, PC-3 cells were added to the monolayer, and the electrical resistance was measured every at specific time intervals (i) and the final measurement at 24 h (ii).



(i)



(ii)

Figure 3.18 Effect of addition of PC-3 cells on trans endothelial electric resistance of MDCK monolayer.

Chapter 4

DISCUSSION

Majority of men who die of prostate cancer have advanced metastatic disease. Metastases to bones in pelvis, femur, and vertebrae are the most common and cause morbidity due to various effects like compression fractures, spinal cord compression, severe pain, and bladder and bowel incontinence to name a few (1-3). Prostate cancer metastases comprises of a series of steps starting with the separation from the primary prostate tumor site, invasion through the basement membrane of the organ, entry into the vasculature (Batson venous plexus), survival in the vasculature by successfully evading the immune mechanisms, entry into bone marrow followed by extravasation through the bone marrow endothelium and entry into the bone stroma and adaptation, survival and growth in the bone. In this cascade, the particular step where tumor cell extravasates across the bone marrow endothelium can be compared to leukocyte diapedesis across vascular endothelium during inflammation. This step can be further divided into multiple sub-steps which include tumor cell arrest and binding to bone marrow endothelial cells, spreading on the endothelium, migration along the endothelial barrier, tumor cell diapedesis (a.k.a. transendothelial cell migration) and invasion of the basal lamina and underlying stromal components. Critical in this process are changes in tumor cell shape and motility regulated by Rho GTPases through cytoskeleton reorganizations.

Rho GTPases are a sub-family of Ras superfamily of small monomeric GTPases that regulate actin cytoskeleton that switch between inactive GDP state to active GTP bound state. This cycle is controlled by different regulatory proteins, such as guanine exchange factors (GEFs), guanine dissociation inhibitors (GDIs) , GTPase activating proteins (GAPs), which in turn the downstream signal transduction and effector molecules(24). Overexpression and aberrant activation of Rho GTPases is observed in many cancers including prostate cancer. Rho GTPases have been shown to play a role in tumorigenesis and metastases. Dynamic reorganization of cytoskeleton is essential for tumor invasion and motility which requires interplay between different Rho GTPases. It has been shown that specific Rho GTPases have distinct functions within a cell and their interplay regulates cell morphology and migration(47-50).

RhoC GTPase overexpression and activation has been observed in different prostate cancer cell lines where it has been shown to be required for tumor invasion(51,52). Down regulation of Rho C GTPase in PC-3 cells either through dominant negative mutation or introduction of shRNA to RhoC led to elongated, fibroblastic morphology and changes in lamellopodia formation which was reminiscent of epithelial to mesenchymal transition(54). This was similar to the changes in morphology observed in CHO.K1 fibroblasts upon deletion of the LD4 domain of paxillin resulting in redistribution of paxillin kinase linker (PKL) to the cytoplasm of the cells. Redistribution of PKL and therefore assembly of focal adhesion complex has been shown to be regulated by RhoC GTPase. The change in morphology upon RhoC downregulation was found to be due to increase in Rac GTPase activation(54).

Rac GTPases have been shown to be important in tumor diapedesis by causing tumor cell to spread and form lamellopodia which acts as a sensor for migration between the endothelial cells. Down-regulation of Rac GTPase in PC-3 cells resulted in drastic changes in tumor cell morphology forming rounded cells with very little lamellopodia formation(57). It also decreased the tumor cells ability to undergo diapedesis across bone marrow endothelium suggesting that while RhoC GTPases is important for PC-3 cell invasion Rac GTPases play a key role during PC-3 extravasation across bone marrow endothelium into bone stroma.

There are four members in the Rac branch of the Rho sub-family, Rac 1, Rac2, Rac3 and RhoG(61-64). Though it is clear that Rac GTPase is important for PC-3 diapedesis across bone marrow endothelium the specific role played by each of these isoforms is not yet clear. This study was aimed at determining the individual roles of the different Rac GTPases in PC-3 diapedesis.

Rac 1 was found to be the most predominant of the Rac isoforms with Rac3 and RhoG present at low levels. This contrasts with the levels reported in a previous study (66) where Rac3 was shown to be the predominant Rac isoform expressed. The difference could be attributed to the fact that the above-mentioned study looked at Rac levels from a prostate cancer tissue at the primary site while PC-3 cells were derived from advanced androgen independent bone metastasized prostate cancer. The tissue derived from primary tumor site also has neuroendocrine component which can explain higher levels of Rac3 since Rac3 is known to be present in large levels in nervous tissue. Also the number of sample studied for measuring Rac1 isoform was a limiting factor in the above-mentioned study. However it is plausible to speculate that the levels of Rac isoforms change during carcinogenesis and

progression through metastatic cascade. Rac2 has been previously shown to be not expressed in prostate cancer.

Measurement of effects of depletion of specific Rac isoforms on total Rac activation in PC-3 cells gave an idea of the relative contribution of each isoform while pointing to the interesting interplay going on between the different isoforms modulating the total Rac activation levels . Depletion of Rac 1 using shRNA to Rac1 caused a marked decrease in total Rac activation suggesting its major contribution to the total Rac activation levels. Depletion of RhoG caused decrease in total Rac activation levels but the effect was not as marked as that of depletion of Rac 1. Interestingly depletion of Rac 3 resulted in an increase in the total Rac activation levels indicating a possible reciprocal relationship between Rac 1 and Rac3 since Rac1 looks like the predominant isoform contributing to the total Rac activation levels. This type of relationship between Rac 1 and Rac 3 is reminiscent of the reciprocal activation observed between RhoA and RhoC in breast cancer cell lines (72).

Further insight into the interplay between different Rac isoforms was gained by studying the role of RhoG in activating Rac1. RhoG is known to share similar signaling molecules and downstream effectors with Rac1. It has been recently shown that RhoG can cause activation of Rac1 by interaction with DOCK-180/ELMO which is a member of the DOCK family of guanine nucleotide exchange factors (GEFs) (67). CCL2(a.k.a MCP-1) , a chemokine secreted by BMEC has been shown to cause Rac1 activation and epithelial to mesenchymal transition in PC-3 cells similar to the change in morphology observed upon downregulation of RhoC. Further CCL2 has been show to cause Rac1 activation through stimulation of PCNT1, a novel actin regulating protein(41,-44,68,69). To test if RhoG acts downstream of PCNT1 to cause

Rac1 activation PC-3 cells were downregulated for RhoG using siRNA and stimulated with CCL2 and total Rac activation measured. The majority of Rac activation levels is represented by Rac 1 activation levels. Downregulation of RhoG in CCL2 stimulated PC-3 cells caused a significant decrease in the amount of total activated Rac levels and this effect was reversed upon introduction of siRNA resistant RhoG. This suggests that activation of Rac1 in PC-3 cells can take place through direct stimulation of Rac GEFs of through activation of RhoG. This implies that though present in low levels in PC-3 cells RhoG is an important Rac isoform by causing Rac1 activation.

Keeping in mind these possible interactions between different Rac isoforms the next step was to study their roles in the process of PC-3 diapedesis across bone marrow endothelium. Diapedesis is a multi-step process as mentioned above, involving PC-3 cell initial rolling, spreading and binding to the bone marrow endothelium cells. To study this, elastic modulus which is an indicator of the amount of cell stiffness, was measured using atomic force microscopy. It was observed that when PC-3 cells were added to BMEC monolayer there was a consistent decrease in the elastic modulus of BMECs suggesting biological interactions resulting in changes in the actin cytoskeleton. PC-3 cells however showed no change in the elastic modulus upon contact with BMECs. When PC-3 cells depleted of Rac1 were added to BMEC there was no decrease in the elastic modulus of BMECs suggesting a role of Rac1 GTPase in the PC-3 BMEC initial interaction mediating changes in actin cytoskeleton. In leukocyte diapedesis, binding to vascular endothelium is mediated through interactions between integrin binding to cellular adhesion molecules on endothelium and it has been shown that Rac GTPase increases surface levels of ICAM-1 on endothelial cells which facilitates tight binding with the integrins on leukocytes (13,

16, 73, 74) .Studies have shown the role of $\beta 1$ –integrin in PC-3 binding to BMECs(9,10, 73, 74 , 75). It is possible that PC-3 binding to BMECs through integrins results in activation of Rac GTPase which causes further activation of integrin through inside out signaling and thus strengthening the interaction. No significant change was observed when Rac-3 or RhoG were downregulated in PC-3 cells and elasticity measured.

In the next step the effect of depletion of each of the isoforms on PC-3 diapedesis across BMEC monolayer was studied using diapedesis assay. Upon depletion of Rac 1 there was a significant decrease in diapedesis. Downregulation of RhoG also caused a slight increase in diapedesis and depletion of Rac3 resulted in a significant increase in PC-3 diapedesis. This can be explained through reciprocal activation of Rac 1 and Rac3 . When Rac3 was depleted there was increase in activated Rac1 levels promoting diapedesis. These effects were reversed upon introduction of siRNA resistant Rac 1, 3 and RhoG. Treatment of PC-3 cells with a pharmacological inhibitor of Rac1 also resulted in a decrease in diapedesis.

In the next step, effect of depletion of Rac isoforms on CCL2 stimulated PC-3 diapedesis was studied. Rac-1 depletion in CCL2 stimulated PC-3 cells resulted in a marked decrease in diapedesis. Downregulation of RhoG in CCL2 stimulated PC-3 cells resulted in a decrease in diapedesis in contrast to the increase in diapedesis observed on RhoG depletion in unstimulated cells. These effects were reversed on introduction of siRNA resistant forms. When fast cycling RhoG (RhoGQ63L) was introduced in Rac1 depleted CCL2 stimulated PC-3 cells there was not much increase in diapedesis indicating that RhoG's effect on PC-3 diapedesis is mediated through activation of Rac1.

Followed by the interaction between PC-3 and BMEC monolayer disruptions of the cellular junctions that maintain the monolayer is required for passage of PC-3 across the endothelium. Rac GTPases are essential for the maintenance of endothelium permeability by regulating the integrity of adherens and tight junctions. At the same time Rac has been shown to facilitate leukocyte diapedesis by increasing ICAM-1 levels on endothelial cells and thus promoting the initial steps in diapedesis(73,77). Therefore the next step was to further understand the role of Rac isoforms in regulation of cell junctions following interactions with PC-3 .

Trans-endothelial electrical resistance (TEER) measurements are conventionally used to study permeability of a cellular monolayer (76). To determine the effect of addition of PC-3 cells on the permeability of BMECs monolayer TEER measurements were used. First the optimal TEER measurement for BMEC was determined to be on day four by growing cells into monolayer using different cell concentration and daily TEER measurements. PC-3 cells in same concentration as BMECs were added to BMEC monolayer grown for four days and TEER was measured at different time points. Drop in TEER readings after addition of PC-3 was noted in the first 10 min which stabilized by 20-30 min continuing till 60 min. TEER returned back to original levels at 24 hour post PC-3 addition. When PC-3 were added to BMECs there was a biological interaction which further resulted in the disruption of BMEC monolayer presumably through disruptions in cellular junctions thus causing increased permeability. This was most evident during the initial 10 minutes after contact of PC-3 on BMEC. After 24 hours there was restoration in TEER which can be explained by restoration of cellular junctions which are known to be dynamic complexes.

To understand better, TEER measurements were narrowed to tighter intervals going on till 30 min after addition of PC-3. It was found that the drop in TEER starts at around 3 min and continues till 10-15 min after which it stabilizes. BMEC monolayer depleted of Rac1 were more permeable indicative of disrupted cellular junctions compared to control and addition of PC-3 cells had no further effect. Depletion of Rac 3 from BMEC monolayer had no effect on the pattern of permeability changes observed on addition of PC-3 cells compared to control. Depletion of RhoG from BMEC monolayer had no effect on the pattern of permeability changes compared to control. Addition of Rac-1 depleted PC-3 cells on BMEC resulted in no fluctuations in permeability which was observed in control while depletion of Rac-3 from PC-3 had similar effect on permeability as control. Depletion of RhoG from PC-3 caused slightly lesser decrease in permeability of BMEC compared to controls.

These findings suggest that Rac1 in both PC-3 and BMEC facilitate PC-3/BMEC interactions through presumably through increased expression of ICAM-1 on BMEC and increased interactions with β integrins on PC-3. Clustering of ICAM in leukocytes results in RhoA/ROCK signaling activation inducing actin-myosin contractions and disruption of membrane permeability (73-77). It is plausible to think of similar mechanisms going on during PC-3/BMEC interactions. It would be interesting to study the effect of downregulation of Rac1 in BMEC on ICAM-1 expression levels and PC3/ BMEC binding. While Rac -1 on BMEC is important to maintain the cellular junctions it is plausible that following PC-3 /BMEC interactions RhoA activation becomes more predominant and mediates the decrease in permeability. This argument is further backed by the observation that down-regulation

of Rac3 in BMEC which increases Rac-1 activation levels does not change the pattern of drop in permeability upon PC-3 addition. Downregulation of RhoG from BMEC seemed to cause no effect on the permeability following addition of PC-3 however depletion in PC-3 resulted in a lesser level of decrease in BMEC permeability observed compared to controls which could be due to reduced levels of Rac1 activation and thus decreased binding to BMEC.

To test if the observed effects of PC-3 on BMEC permeability were endothelium specific, effect of PC-3 cells on MDCK cells monolayer permeability was studied. Addition of PC-3 cells on MDCK monolayer resulted in continuously increasing TEER readings indicative of no changes in the cellular junctions. This effect continued even after 24 hours of addition of PC-3 cells. This suggests that PC-3 has endothelium specific interactions with BMECs(10,35). This supports the established notion of the preferential skeletal metastases of prostate cancer due to specific interactions between prostate cancer and bone marrow endothelium.

Chapter 5

CONCLUSION

In summary, the present study highlights the role of different Rac isoforms in PC-3 diapedesis across bone marrow endothelium into bone stroma. The following conclusions can be drawn from the study:

- Rac1 is the predominant Rac-isoform in PC-3 cells
- RhoG causes activation of Rac1 on CCL2 stimulated PC-3 levels . Interaction of CCL2 with its receptor causes activation of PCNT1, a novel actin regulating protein , which further interacts with RhoGEFs which in turn causes causes hierarchical activation of Rac1 through interaction with DOCK-180 ELMO
- Rac 1 and Rac3 have reciprocal relationship in that downregulation of Rac3 increases Rac1 activation levels.
- Rac1 in PC-3 is important in mediating binding interactions with BMECs while Rac1 in BMEC presumably facilitates expression of ICAM-1 levels and interactions with β 1 integrin on PC-3.
- Rac-1 maintains BMEC monolayer integrity and its downregulation results in increase in permeability.
- Downregulation of Rac-3 in PC-3 increases diapedesis by increasing Rac-1 activation and thus PC-3/BMEC interactions.
- Downregulation of Rac3 or RhoG does not affect permeability of BMEC.

- PC-3/endothelial interactions are endothelium specific with decreased permeability observed on interactions with BMEC while no affect on permeability was noted on interaction with MDCK cells.

For further study, it would be interesting to measure the levels of ICAM-1 upon Rac isoform depletion in BMEC and its effect on PC-3 binding. It appears that PC-3 diapedesis across BMEC mimics leukocyte diapedesis during inflammation; therefore it is quite possible to observe similar cellular mechanisms mediating the process. Also it would be interesting to study the role of Rac isoforms in sensing and modulation of cell to cell junction in BMEC monolayer.

Lastly, this was an in-vitro study and it would be interesting to attempt replicating the findings to an in-vivo model using animals. Rac-1 depletion is known to be lethal during embryogenesis; perhaps a conditional gene knockout using Cre-Lox recombination can be attempted.

REFERENCES

1. Nelson WG, Marzo AM, Isaacs WB, 2003 , Prostate Cancer , New England Journal of Medicine , 349 366–381.
2. Jemal, A., Siegel, R., Xu, J. and Ward, E. (2010), Cancer Statistics, 2010. CA: A Cancer Journal for Clinicians, 60: 277–300. doi: 10.3322/caac.20073
3. Keller, E. T. and Brown, J. (2004), Prostate cancer bone metastases promote both osteolytic and osteoblastic activity. Journal of Cellular Biochemistry, 91: 718–729. doi: 10.1002/jcb.10662
4. Abrams H, Spiro R, Goldstein N. 1950. Metastases in carcinoma. *Cancer* **3**: 74–85.
5. Rana A, Chisholm GD, Khan M, Sekharjit SS, Merrick MV, Elton RA. 1993. Patterns of bone metastasis and their prognostic significance in patients with carcinoma of the prostate. *Br J Urol* **72**: 933–936.
6. Coleman RE. 1997. Skeletal complications of malignancy. *Cancer* **80**: 1588–1594.
7. Szostak MJ, Kyprianou N. 2000. Radiation-induced apoptosis: Predictive and therapeutic significance in radiotherapy of prostate cancer (review). *Oncol Rep* **7**: 699-706
8. Lehr JE, Pienta KJ. Preferential adhesion of prostate cancer cells to a human bone marrow endothelial cell line. Journal of the National Cancer Institute. 1998;90(2):118–123.
9. Cooper CR, McLean L, Mucci NR, Poncza P, Pienta KJ. Prostate cancer cell adhesion to quiescent endothelial cells is not mediated by beta-1 integrin subunit. Anticancer Research. 2000;20(6 B):4159–4162. [PubMed]

10. Cooper CR, McLean L, Walsh M, et al. Preferential adhesion of prostate cancer cells to bone is mediated by binding to bone marrow endothelial cells as compared to extracellular matrix components in vitro. *Clinical Cancer Research*. 2000;6(12):4839–4847. [PubMed]
11. Batson OV (1940 Jul). "The function of the vertebral veins and their role in the spread of metastasis". *Annals of Surgery* **112** (1): 138–49.
12. Fayth L. Miles, Freddie L. Pruitt, Kenneth L. van Golen, Carlton R. Cooper "Stepping out of the flow: capillary extravasation in cancer metastasis" *Clin Exp Metastasis* (2008) 25:305–324
13. Zimmerman GA, Prescott SM, McIntyre TM (1992) Endothelial cell interactions with granulocytes: tethering and signaling molecules. *Immunol Today* 13:93–100
14. McIntyre TM, Prescott SM, Weyrich AS, Zimmerman GA (2003) Cell–cell interactions: leukocyte–endothelial interactions. *Curr Opin Hematol* 10:150–158
15. Oppenheimer-Marks N, Davis LS, Bogue DT, Ramberg J, Lipsky PE (1991) Differential utilization of ICAM-1 and VCAM-1 during the adhesion and transendothelial migration of human T lymphocytes. *J Immunol* 147:2913–2921
16. Reiss Y, Engelhardt B (1999) T cell interaction with ICAM-1-deficient endothelium in vitro: transendothelial migration of different T cell populations is mediated by endothelial ICAM-1 and ICAM-2. *Int Immunol* 11:1527–1539
17. Wong D, Prameya R, Dorovini-Zis K (1999) In vitro adhesion and migration of T lymphocytes across monolayers of human brain microvessel endothelial cells: regulation by ICAM-1, VCAM-1, E-selectin and PECAM-1. *J Neuropathol Exp Neurol* 58:138–152

18. Ostermann G, Weber KS, Zerneck A, Schroder A, Weber C (2002) JAM-1 is a ligand of the beta(2) integrin LFA-1 involved in transendothelial migration of leukocytes. *Nat Immunol* 3:151–158
19. Greenwood J, Wang Y, Calder VL (1995) Lymphocyte adhesion and transendothelial migration in the central nervous system: the role of LFA-1, ICAM-1, VLA-4 and VCAM-1. *off. Immunology* 86:408–415
20. Reinhardt PH, Elliott JF, Kubes P (1997) Neutrophils can adhere via alpha4beta1-integrin under flow conditions. *Blood* 89: 3837–3846
21. Sandig M, Negrou E, Rogers KA (1997) Changes in the distribution of LFA-1, catenins, and F-actin during transendothelial migration of monocytes in culture. *J Cell Sci* 110(Pt 22): 2807–2818
22. Pawlowski NA, Kaplan G, Abraham E, Cohn ZA (1988) The selective binding and transmigration of monocytes through the junctional complexes of human endothelium. *J Exp Med* 168:1865–1882
23. Engelhardt B, Wolburg H (2004) Mini-review: transendothelial migration of leukocytes: through the front door or around the side of the house? *Eur J Immunol* 34:2955–2963
24. Bishop AL, Hall A (2000) Rho GTPases and their effector proteins. *Biochem J* 348 (Pt 2):241–255
25. Braga VM, Del Maschio A, Machesky L, Dejana E (1999) Regulation of cadherin function by Rho and Rac: modulation by junction maturation and cellular context. *Mol Biol Cell* 10:9–22
26. Braga VM (2002) Cell–cell adhesion and signalling. *Curr Opin Cell Biol* 14:546–556

27. Sahai E, Marshall CJ (2002) ROCK and Dia have opposing effects on adherens junctions downstream of Rho. *Nat Cell Biol* 4:408–415
28. Su WH, Chen HI, Jen CJ (2002) Differential movements of VEcadherin and PECAM-1 during transmigration of polymorphonuclear leukocytes through human umbilical vein endothelium. *Blood* 100:3597–3603
29. Luscinskas FW, Ma S, Nusrat A, Parkos CA, Shaw SK (2002) The role of endothelial cell lateral junctions during leukocyte trafficking. *Immunol Rev* 186:57–67
30. Shaw SK, Bamba PS, Perkins BN, Luscinskas FW (2001) Realtime imaging of vascular endothelial–cadherin during leukocyte transmigration across endothelium. *J Immunol* 167:2323–2330
31. Etienne S, Adamson P, Greenwood J et al (1998) ICAM-1 signaling pathways associated with Rho activation in microvascular brain endothelial cells. *J Immunol* 161:5755–5761
32. Takahashi K, Sasaki T, Mammoto A et al (1997) Direct interaction of the Rho GDP dissociation inhibitor with ezrin/radixin/ moesin initiates the activation of the Rho small G protein. *J Biol Chem* 272:23371–23375
33. Barreiro O, Yanez-Mo M, Serrador JM et al (2002) Dynamic interaction of VCAM-1 and ICAM-1 with moesin and ezrin in a novel endothelial docking structure for adherent leukocytes. *J Cell Biol* 157:1233–1245
34. Heiska L, Alfthan K, Gronholm M et al (1998) Association of ezrin with intercellular adhesion molecule-1 and -2 (ICAM-1 and ICAM-2). Regulation by phosphatidylinositol 4, 5-bisphosphate. *J Biol Chem* 273:21893–21900

35. Cooper CR, McLean L, Walsh M et al (2000) Preferential adhesion of prostate cancer cells to bone is mediated by binding to bone marrow endothelial cells as compared to extracellular matrix components in vitro. *Clin Cancer Res* 6:4839–4847
36. Haq M, Goltzman D, Tremblay G, Brodt P (1992) Rat prostate adenocarcinoma cells disseminate to bone and adhere preferentially to bone marrow-derived endothelial cells. *Cancer Res* 52:4613–4619
37. Lehr JE, Pienta KJ (1998) Preferential adhesion of prostate cancer cells to a human bone marrow endothelial cell line. *J Natl Cancer Inst* 90:118–123
38. Scott LJ, Clarke NW, George NJ et al (2001) Interactions of human prostatic epithelial cells with bone marrow endothelium: binding and invasion. *Br J Cancer* 84:1417–1423
39. Glinsky VV, Glinsky GV, Rittenhouse-Olson K et al (2001) The role of Thomsen–Friedenreich antigen in adhesion of human breast and prostate cancer cells to the endothelium. *Cancer Res* 61:4851–4857
40. Romanov VI, Goligorsky MS. 1999. RGD-recognizing integrins mediate interactions of human prostate carcinoma cells with endothelial cells in vitro. *Prostate* 39: 108-118.
41. Ohta M, Kitadai Y, Tanaka S, Yoshihara M, Yasui W, Mukaida N, Haruma K, Chayama K. 2002. Monocyte chemoattractant protein-1 expression correlates with macrophage infiltration and tumor vascularity in human esophageal squamous cell carcinomas. *Int J Cancer* 102: 220-224.
42. Balkwill F. 2003. Chemokine biology in cancer. *Semin Immunol* 15:49-55.
43. Loberg RD, Day LL, Harwood J, Ying C, St John LN, Giles R, Neeley CK, Pienta KJ. 2006. CCL2 is a potent regulator of prostate cancer cell migration and

proliferation. *Neoplasia* 8:578-586.

44. Loberg RD, Tantivejkul K, Craig M, Neeley CK, Pienta KJ. 2007. PAR1-mediated RhoA activation facilitates CCL2- induced chemotaxis in PC-3 cells. *J Cell Biochem* 101: 1292-1300.

45. van Golen KL, Ying C, Sequeira L, Dubyk CW, Reisenberger T, Chinnaiyan AM, Pienta KJ, Loberg RD (2008) CCL2 induces prostate cancer transendothelial cell migration via activation of the small GTPase Rac. *Journal of Cellular Biochemistry* 104:1587-1597

46. Chapter 1, emanuel vignal et al , Marc Symmons, Rho GTPase

47. Etienne- Manneville and A. Hall, Rho GTPases in cell biology *Nature*, **420** (2002), pp. 629–635. [SD-008]

48. Geyer M and Wittinghofer A (1997). GEFs, GAPs, GDIs and effectors: taking a closer (3D) look at the regulation of Ras-related GTP-binding proteins. *Curr Opin Struct Biol* 7, 786-792.

49. Hall A. Rho GTPases and the actin cytoskeleton. *Science*. 1998;279(5350):509–514.

50. Sahai E, Marshall CJ. RHO-GTPases and cancer. *Nature Reviews Cancer*. 2002;2(2):133–142.

51. Wennerberg K, Der CJ. Rho-family GTPases: it's not only Rac and Rho (and i like it) *Journal of Cell Science*. 2004;117(8):1301–1312

52. Yao H, Dashner EJ, van Golen CM, van Golen KL. RhoC GTPase is required for PC-3 prostate cancer cell invasion but not motility. *Oncogene*. 2006;25(16):2285–2296.

53. van Golen KL, Ying C, Sequeira L, et al. CCL2 induces prostate cancer transendothelial cell migration via activation of the small GTPase rac. *Journal of Cellular Biochemistry*. 2008;104(5):1587–1597.
54. Sequeira L, Dubyk CW, Riesenberger TA, Cooper CR, van Golen KL. Rho GTPases in PC-3 prostate cancer cell morphology, invasion and tumor cell diapedesis. *Clinical and Experimental Metastasis*. 2008;25(5):569–579
55. Hall CL, Dai JL, van Golen KL, Keller ET, Long MW. Type I collagen receptor ($\alpha 2 \beta 1$) signaling promotes the growth of human prostate cancer cells within the bone. *Cancer Research*. 2006;66:8648–8654.
- 56.. Hall CL, Dubyk CW, Riesenberger TA, et al. Type I collagen receptor ($\alpha\beta$) signaling promotes prostate cancer invasion through RhoC GTPase. *Neoplasia*. 2008;10(8):797–803
- 57 Nobes CD, Hall A. Rho, Rac, and Cdc42 GTPases regulate the assembly of multimolecular focal complexes associated with actin stress fibers, lamellipodia, and filopodia. *Cell*. 1995;81(1):53–62.
58. Hajdo-Milasinovic A, Ellenbroek SIJ, van Es S, van der Vaart B, Collard JG. Rac1 and Rac3 have opposing functions in cell adhesion and differentiation of neuronal cells. *Journal of Cell Science*. 2007;120(4):555–566.

59. Gualdoni S, Albertinazzi C, Corbetta S, Valtorta F, de Curtis I. Normal levels of Rac1 are important for dendritic but not axonal development in hippocampal neurons. *Biology of the Cell*.2007;99(8):455–464.
60. Chan A-Y, Coniglio SJ, et al. Roles of the Rac1 and Rac3 GTPases in human tumor cell invasion.*Oncogene*. 2005;24(53):7821–7829.
61. Olson MF, Ashworth A & Hall A 1995 An essential role for Rho, Rac, and Cdc42 GTPases in cell cycle progression through G1. *Science* 269 1270–1272
62. Hordijk PL, ten Klooster JP, van der Kammen RA, Michiels F, Oomen LC & Collard JG 1997 Inhibition of invasion of epithelial cells by Tiam1-Rac signaling. *Science* 278 1464–1466
63. Kuroda S, Fukata M, Nakagawa M, Fujii K, Nakamura T, Ookubo T, Izawa I, Nagase T, Nomura N, Tani H *et al.* 1998 Role of IQGAP1, a target of the small GTPases Cdc42 and Rac1, in regulation of E-cadherin-mediated cell–cell adhesion. *Science* **281** 832–835.
64. Keith Burridge, Krister Wennerberg , Rho and Rac Take Center Stage, *Cell*, Volume 116, Issue 2, 23 January 2004, Pages 167-179
65. Mark A Barber, Heidi CE Welch, PI3K and RAC signalling in leukocyte and cancer cell migration , *Electronic Journal of Oncology, Bulletin du Cancer*. Volume 93, Number 5, 10044-52, Mai 2006
66. Engers R, Ziegler S, Mueller M, Walter A, Willers R, Gabbert HE. Prognostic relevance of increased Rac GTPase expression in prostate carcinomas. *Endocrine-Related Cancer*.2007;14(2):245–256.
67. Wennerberg K, Ellerbroek SM, et al. RhoG signals in parallel with Rac1 and Cdc42. *The Journal of Biological Chemistry*. 2002;277(49):47810–47817.

- 68.. Katoh H, Negishi M. RhoG activates Rac1 by direct interaction with the Dock180-binding protein Elmo. *Nature*. 2003;424(6947):461–464.
69. Katoh H, Hiramoto K, Negishi M. Activation of Rac1 by RhoG regulates cell migration. *Journal of Cell Science*. 2006;119(1):56–65.
70. van Golen KL, Wu ZF, Qiao XT, Bao LW, Merajver SD. RhoC GTPase overexpression modulates induction of angiogenic factors in breast cells. *Neoplasia*. 2000;2(5):418–425.
71. Chan A-Y, Coniglio SJ, et al. Roles of the Rac1 and Rac3 GTPases in human tumor cell invasion. *Oncogene*. 2005;24(53):7821–7829.
- 72 Francisco M. Vega, Gilbert Fruhwirth, Tony Ng, Anne J. Ridley , RhoA and RhoC have distinct roles in migration and invasion by acting through different targets *J. Cell Biol.*2011;193:655-665, May 16, 2011 (10.1083/jcb.201011038).
73. Eva Cernuda-Morollón, Anne J. Ridley, Rho GTPases and Leukocyte Adhesion Receptor Expression and Function in Endothelial Cells, *Circulation Research*.2006; 98: 757-767
74. Witkowski CM, Rabinovitz I, Nagle RB, Affinito KSD, Cress AE. Characterization of integrin subunits, cellular adhesion and tumorigenicity of four human prostate cell lines. *Journal of Cancer Research and Clinical Oncology*. 1993;119(11):637–644.
75. Dedhar S, Saulnier R, Nagle R, Overall CM. Specific alterations in the expression of alpha 3 beta 1 and alpha 6 beta 4 integrins in highly invasive and metastatic variants of human prostate carcinoma cells selected by in vitro invasion through reconstituted basement membrane. *Clinical and Experimental Metastasis*. 1993;11:391–400.

76. Tretiach, Marina, Transendothelial electrical resistance of bovine retinal capillary endothelial cells is influenced by cell growth patterns: an ultrastructural study, *Clinical & Experimental Ophthalmology*, Vol. 31, No. 4, 2003, pp. 348-348-353.
77. Wójciak-Stothard B, Potempa S, Eichholtz T, Ridley AJ. Rho and Rac but not Cdc42 regulate endothelial cell permeability. *J Cell Sci.* 2001 Apr;114(Pt 7):1343-55.
78. S. Suresh, J. Spatz, J. P. Mills, et al., "Connections between single-cell biomechanics and human disease states: gastrointestinal cancer and malaria," *Acta Biomaterialia*, vol. 1, no. 1, pp. 15–30, 2005.